Receiver Windowing Design for Narrowband Interference Mitigation in MB-OFDM UWB System

by Zixia Hu

Delft University of Technology, March 2009

A thesis submitted to the Electrical Engineering, Mathematics and Computer Science Department of Delft University of Technology in partial fulfillment of the requirements for the degree of **Master of Science.**

Supervisor: dr. ir. Alle-Jan van der Veen
Supervisor: Maurice Stassen, Ajay Kapoor

Delft University of Technology, the Netherlands

Approval

Name: Zixia Hu

Degree: Master of Science

Title of Thesis: Receiver Windowing Design for Narrowband
                   Interference Mitigation in MB-OFDM UWB System

Committee in Charge of Approval:

Chair: _____

                Professor Alle-Jan van der Veen
                Department of Electrical Engineering

Committee member: _____

                   Professor Geert Leus
                Department of Electrical Engineering

                   _____
                   Professor Gerard Janssen
                Department of Electrical Engineering

Abstract

In 2005, the WiMedia Alliance working with the European Computer Manufacturers Association (ECMA) announced the establishment of the WiMedia MB-OFDM (Multiband Orthogonal Frequency Division Multiplexing) UWB radio platform as their global UWB standard. It was also chosen as the physical layer (PHY) of high data rate wireless specifications for high speed Wireless USB (W-USB), Bluetooth 3.0 and Wireless High-Definition Media Interface (HDMI). However, due to the low power and wide bandwidth nature of UWB systems, in-band narrowband interference (NBI) may hinder the receiver performance.

This thesis presents an analysis of NBI impact on the MB-OFDM system for UWB communication. The intent of our analysis is to provide practical solutions for interference mitigation under different NBI models. In our work, a new receiver windowing for zero padding (ZP) OFDM system is proposed to reduce NBI spreading in the MB-OFDM UWB system. Simulations demonstrate the effectiveness of windowing under different NBI models.

Contents

Illustrations

LIST OF ACRONYMS

AWGN Additive White Gaussian Noise
bps Bits per second
CRC Cyclic Redundancy Check
CP Cyclic Prefix
dB Decibel (ratio in log scale)
dBm Decibel relative to 1 milliwatt
DCM Dual Carrier Modulation
DFT Discrete Fourier Transform
FDS Frequency-Domain Spreading
FEC Forward Error Correction
FFI Fixed-Frequency Interleaving
FFT Fast Fourier Transform
GHz Gigahertz
GSM Global System for Mobile
Communications
HDMI High-Definition Media Interface
ICI Inter-carrier Interference
IDFT Inverse Discrete Fourier
Transform
IFFT Inverse Fast Fourier Transform
ISI Inter-symbol Interference
MAC Medium Access Control
Multi-Band OFDM Alliance (MBOA)
MB-OFDM Multi-Band Orthogonal
Frequency division multiplexing
OFDM Orthogonal Frequency Division
Multiplexing

PAN Personal Area Network
PDU Protocol Data Unit
PER Packet error rate
PHY Physical layer
PLCP Physical Layer Convergence
Protocol
PPDU PLCP Protocol Data Unit
PSD Power Spectral Density
PSDU PLCP Service Data Unit
PSK Phase Shift Keying
QAM Quadrature Amplitude Modulation
QPSK Quadrature Phase Shift Keying
RF Radio Frequency
RMS Root-mean-squared
SIR Signal-to-interference Ratio
SNR Signal-to-noise Ratio
TDS Time-Domain Spreading
TF Time-Frequency
TFC Time-Frequency Code
TFI Time-Frequency Interleaving
WLAN Wireless Local Area Network
WPAN Wireless Personal Area Network
WSS Wide-sense Stationary
UWB Ultra Wideband
WPAN Wireless Personal Area Network
ZPS Zero Padded Suffix

Acknowledgements

I would like to express my heartfelt gratitude to Prof. dr. ir. Alle-Jan van der Veen, my supervisor in Delft University of Technology, for his constant guidance and time dedicated to my work in the past one year. The monthly technical discussions with him and his visits to the company gave me a lot of help and encouragement.

I would like to express my warmest gratitude to Maurice Stassen and Ajay Kapoor, my supervisors from company (ST-Ericsson), for providing me with valuable advices and instructions in the past ten months. They have guided me through all the stages of the research work and thesis writing. Without their consistent and illuminating guidance, this thesis could not have reached its present form.

I also owe my sincere gratitude to my friends Weiwei Jin, Yuanyuan Bian and Ying Gao, who spent many hours of the thesis proof reading.

Finally, I greatly appreciate my parents' support and endless love. My heart swells with gratitude to all the people who helped me.

Chapter 1.   Introduction

In the near future, with the increment of high speed wireless applications such as Wireless USB (W-USB) and Wireless High-Definition Media Interface (HDMI), the demand for indoor wireless personal area network (WPAN) communication will increase. Among different new technologies which aimed to provide high data rate wireless links, Ultra Wide Band (UWB) is gathering interests as a short-reach transmission system, because it can fulfill the requirements for low transmission power and high-speed digital home networks. Currently, various researches on UWB systems for high data rate transmission in the indoor wireless channel environment are investigated all over the world. One of them, the Multi-Band Orthogonal Frequency division multiplexing (MB-OFDM) based UWB system has been proposed by the Multi-Band OFDM Alliance (MBOA) to provide high data rate wireless communication [1]. The MB-OFDM UWB system is supported by a lot of associations and business organizations due to the low transmission power and high data rate transmission. In recent years, MB-OFDM system has been used in various fields such as wireless personal area networks delivering high speed (480 Mb/s), low power multimedia capabilities for the PC, consumer electronics, mobile, and automotive market segments.

1.1   Motivation and Problem Statement

Low transmission power and huge bandwidth are two characteristics of UWB communications. Since the Federal Communications Commission (FCC) authorizes the unlicensed use of UWB communications in 3.1-10.6GHz, there can be transmission signals (or higher order harmonics) from other wireless systems sharing the same frequency band. If part of the spectrum of MB-OFDM UWB system is overlapped by a relatively strong and narrow band transmission signal, this transmission signal is called narrowband interference (NBI) in the MB-OFDM UWB system. For example, in a UWB-enabled mobile phone as shown in Figure 1.1, the transmitter of Global System for Mobile communications (GSM) signal is very close to the UWB signal receiver. As a result, UWB signal is influenced by the GSM harmonics (generated by the nonlinearity characteristic of the power amplifier (PA)). Due to the spectral leakage effect caused by Fast Fourier transform (FFT) demodulation at OFDM receiver, many subcarriers near the NBI frequency will suffer serious signal to interference ratio (SIR) degradation. In this thesis, the research work is focused on the NBI mitigation in the MB-OFDM UWB system. We consider the following research questions:

• What is NBI in the MB-OFDM UWB system and where does the NBI come from? How can different NBI sources be modeled in the MB-OFDM UWB system? What impact will it have on the MB-OFDM UWB system?

• Are there some existing NBI cancellation/mitigation approaches which can be applied to the MB-OFDM UWB system? If so, what are the advantages and limitations of each approach?

2

• Is it possible to develop a new NBI cancellation/mitigation algorithm for MB-OFDM UWB system?
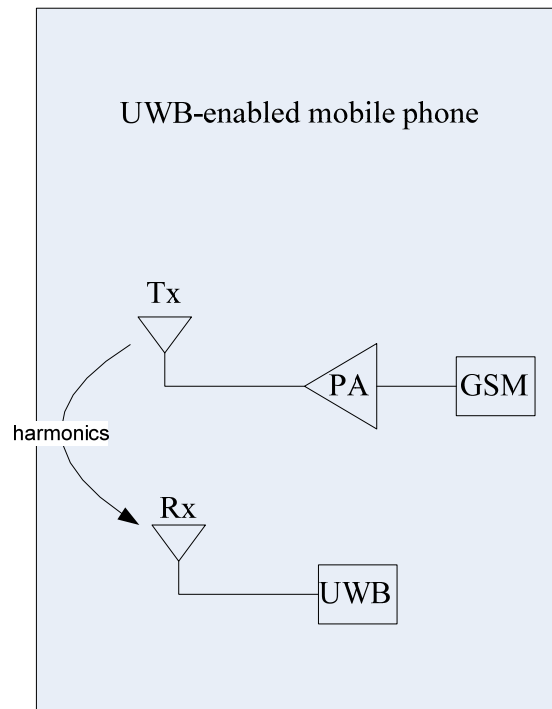
Figure1.1 NBI impact in the UWB-enabled mobile phone

1.2   Thesis Goals

• Model different narrowband interferers in the MB-OFDM UWB system. Analyze the impact of NBI using mathematical reasoning and simulation tools (Matlab).

• Investigate the existing NBI cancellation/mitigation approaches for MB-OFDM UWB system. Compare them and analyze their advantages and limitations.

• Develop a new NBI cancellation/mitigation algorithm to combat strong NBI in MB-OFDM UWB system.

1.3   Organization of Thesis

This thesis consists of seven chapters.

Chapter 2 describes the basic elements of a baseband OFDM system with signal processing aspects.

In Chapter 3, a brief introduction of ECMA-368 MB-OFDM UWB system is given first. Then, common module of MB-OFDM UWB system is explained.

Chapter 4 discusses the NBI interferer models and explains the principle of spectrum leakage first. Then, the impairments introduced by NBI on MB-OFDM UWB system are analyzed. Additionally, four existing NBI cancellation/mitigation techniques for the MB-OFDM UWB system are introduced. Finally, a comprehensive comparison among these techniques is presented.

In Chapter 5, the windowing design objectives are discussed first. Then the traditional rectangular window and three testing windowing schemes for ZP-OFDM system are analyzed. Finally, a new receiver windowing design (a windowing operation before FFT at the receiver) for MB-OFDM UWB system which adopts zero padded (ZP)-OFDM scheme is given.

Chapter 6 introduces additive white Gaussian noise (AWGN) channel model and IEEE 802.15.3a channel models first. Then, the packet error rate (PER) requirement and confidence interval for MB-OFDM UWB system are introduced. Finally, the packet error rate (PER) performance of the MB-OFDM UWB system in the presence of NBI (GSM and Wireless LAN harmonics) under different channel models is presented, respectively.

The thesis is concluded in Chapter 7 which summarizes the thesis and discusses future research work.

References

[1] IEEE 802.15 High Rate Alternative PHY Task Group (TG3a) for wireless Personal Area Networks, "Multi-Band OFDM Physical Layer Proposal for IEEE 802.15.3a Task Group 3a", IEEE P802.15-03/268r3

Chapter 2.   An overview of OFDM Technology

In chapter 1, we briefly discussed the NBI spectral leakage problem in the MB-OFDM UWB system. This problem is caused by the FFT demodulation at OFDM receiver (detailed explanation will be presented in chapter 4), therefore it is necessary to introduce the basic principles of OFDM technology which is relevant to our research topic before investigating the NBI mitigation approaches. In this chapter, a baseband OFDM system model is given and common components of the baseband OFDM systems are explained.

2.1   Digital Baseband OFDM System Model

A block diagram of a digital baseband OFDM system is given in Figure 2.1. First the binary bits generated from the data generator are mapped to the constellation points to obtain data symbols. Then the serial data symbols are converted to parallel and Inverse Fast Fourier Transform (IFFT) is applied to these parallel blocks to obtain the time domain OFDM symbols. Later, the OFDM symbols are converted to serial samples again and added guard intervals (GI), such as cyclic prefix (CP) and zero padding (ZP). Then the time-domain OFDM symbols are transmitted through the channel. In the receiver side, the cyclic prefix or zero padding is removed first, and then the signal is transformed to the frequency domain using Fast Fourier Transform (FFT) operation. Finally, the symbols are equalized and demapped to obtain the transmitted information bits.
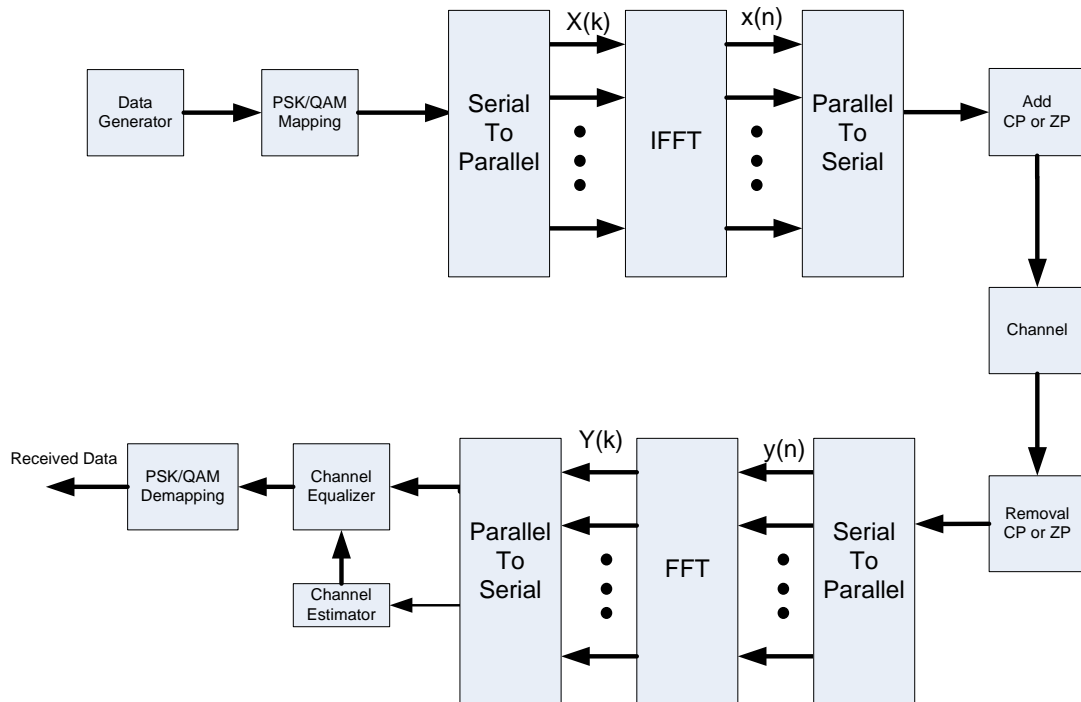
Figure2.1 Block diagram of a digital baseband OFDM system

2.2   PSK/QAM Mapping and Demapping

In the transmitter side, the binary bits stream generated by data generator (as shown in Figure 2.1) will be mapped to the frequency domain (constellation mapping) when they are allocated on each subcarrier. The data stream is mapped using one or more digital modulation schemes, such as Phase-Shift Keying (PSK), Quadrature Amplitude modulation (QAM) [1] etc, which are represented by a complex In-phase and Quadrature-phase (IQ) vector. At the receiver end, the constellation points are demapped to obtain the time domain transmitted information bits.

2.3   Serial to Parallel/ Parallel to Serial Conversion

Data is typically transmitted in the form of a serial data stream, therefore in OFDM systems a serial to parallel conversion block is needed to convert the input serial bit stream to the data in each OFDM symbol. The data allocated to each symbol depends on the modulation scheme used and the number of subcarriers. For example, for a subcarrier modulation of 16-QAM each subcarrier carries 4 bits of data, and for a transmission using 100 subcarriers, the number of bits per symbol would be 400. At the receiver, the parallel to serial conversion block is doing an inverse operation, converting the data in each OFDM symbol to the output serial bit stream.

2.4   IFFT/FFT

In the transmitter side, after serial data stream are converted to parallel blocks of size N, the inverse discrete Fourier transform (IFFT) operation is used to convert modulated data on each subcarrier from frequency domain to the time domain, allowing it to be transmitted. In Figure 2.1, it shows the IFFT operation. Time domain samples are calculated as:

$$x(n) = IFFT\{X(k)\}$$
$$= \sum_{k=0}^{N-1} X(k)e^{j2\pi nk/N} \qquad 0 \le n \le N-1 \qquad (2.1)$$

where $X(k)$ is the symbol transmitted on the kth subcarrier and N is the number of subcarriers. The samples $x(n)$ are interpreted as time domain signal. At the receiver side, the signal is transformed to the frequency domain using FFT operation.

2.5   Equalization

The aim of equalization is to find an inverse filter that compensates for the ISI so that all the multipath signals become shifted and aligned in time, rather than being spread out. In the OFDM systems, the bandwidth of the subcarriers is much narrower than the entire frequency selective fading channel; this makes the frequency response over the bandwidth of each subcarrier effectively flat. As a result, only simple frequency domain equalization is required, in the simulation we use zero-forcing equalization algorithm [2].

2.6 Cyclic prefix and Zero Padding

Cyclic prefix (CP) and zero padding (ZP) are two common guard intervals (GI) in the OFDM system to combat the effect of multipath. As mentioned in chapter 1, the low transmission power is one of the most important characteristics of UWB communications. For this consideration, MB-OFDM UWB system adopts the ZP-OFDM scheme to lower the transmission power (ZP part does not occupy any energy). ZP-OFDM scheme also has another advantage compared to CP-OFDM; it guarantees the symbol recovery and assures the equalization of FIR channels regardless of the channel zero locations [3]. However, the ZP-OFDM scheme increases the receiver complexity. In the following part, the detailed differences between CP-OFDM and ZP-OFDM are discussed.

First let us define the *cyclic property* of CP-OFDM symbol. In CP-OFDM symbol, the basic idea is to replicate part of the OFDM time-domain symbol from back to the front to create a guard period, as shown in the Figure2.2. Time domain OFDM signal is cyclically extended to mitigate the effect of multipath.
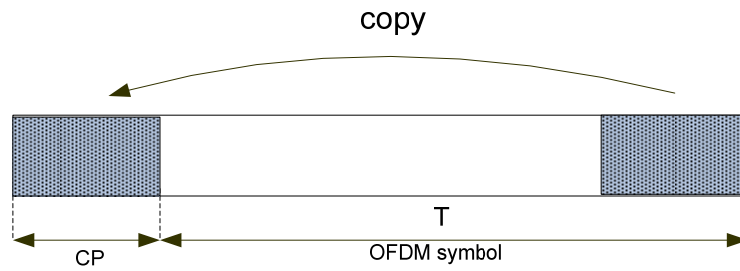
Figure2.2 CP-OFDM symbol

Suppose we have two multipath components, one OFDM symbol contains 4 data including one cyclic-prefix, in the time domain we can see: prefixing the end of the symbol to the beginning makes the linear convolution with channel appear as though it were circular convolution, as shown in equation 2.2.

$$\begin{bmatrix} y_0 \\ y_1 \\ y_2 \end{bmatrix} = \begin{bmatrix} h_1 & h_0 & & \\ & h_1 & h_0 & \\ & & h_1 & h_0 \end{bmatrix} \begin{bmatrix} x_2 \\ \hline x_0 \\ x_1 \\ x_2 \end{bmatrix} = \begin{bmatrix} h_0 & & h_1 \\ h_1 & h_0 & \\ & h_1 & h_0 \end{bmatrix} \begin{bmatrix} x_0 \\ x_1 \\ x_2 \end{bmatrix} \Leftrightarrow y = H_c x \qquad (2.2)$$

$$\Rightarrow \begin{cases} y_0 = h_0 x_0 + h_1 x_2 \\ y_1 = h_0 x_1 + h_1 x_0 \\ y_2 = h_0 x_2 + h_1 x_1 \end{cases} \qquad (2.3)$$

where H_c is a circulant matrix.

From equation 2.3 it can observed, in CP-OFDM symbol every output bit is not only dependent on the current input bit, but also related to the previous input bit. This cyclical

dependency is called *cyclic property*. At the receiver side of CP-OFDM system, after FFT operation, the frequency-domain symbol $Y(k)$ in Figure 2.1 is:

$$Y = Fy = FH_c x = FH_c F^H X = \Lambda X \tag{2.4}$$

where F is the FFT matrix, F^H is the IFFT matrix. Λ is a diagnose matrix .

$$\Lambda = \begin{pmatrix} H_1 & \cdots & \cdots \\ \vdots & \ddots & \vdots \\ \vdots & \cdots & H_n \end{pmatrix}$$

The circulant matrix H_c is diagonalized by the FFT matrix and IFFT matrix, as shown in equation 2.4. The circulant matrix generated by the *cyclic property* of CP-OFDM symbol makes a linear relationship between $X(k)$ (frequency-domain symbols after constellation mapping at the transmitter) and $Y(k)$ (frequency-domain symbol after FFT at the receiver) in Figure 2.1. As a result, only one order frequency domain equalization is required in the CP-OFDM, such as zero-forcing equalization.

Then let us consider the ZP-OFDM symbol case. Figure2.3 shows the ZP-OFDM symbols, ZP part is appended to the time domain OFDM signal. The length of zero padding has to exceed the maximum excess delay of the channel in order to avoid inter symbol interference (ISI) [2]. In Figure2.3, $X[n]$ refers to the nth bit of one ZP-OFDM symbol. At the receiver side of system, ZP-OFDM signal affected by multipath is received. The multipath channel model can be viewed as a finite impulse response (FIR) filter.
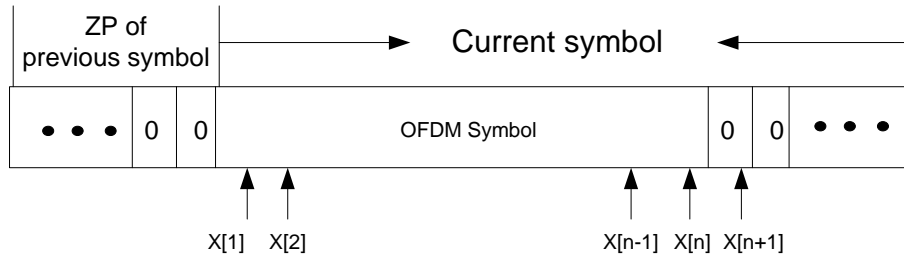
Figure2.3 ZP-OFDM symbols

Suppose we have three multipath components h_1, h_2, and h_3, It can be concluded that the first two samples $X[1]$ and $X[2]$ (as shown in Figure 2.3) at the beginning of current OFDM symbol have already lost the *cyclic property* mentioned in the CP-OFDM case. Let us take the first sample $X[1]$ as an example to demonstrate the conclusion: Figure 2.4 shows the first output $X_{out}[1]$ after multipath:

$$X_{out}[1] = X[1] \cdot h\_1 + 0 \cdot h\_2 + 0 \cdot h\_3 \tag{2.5}$$
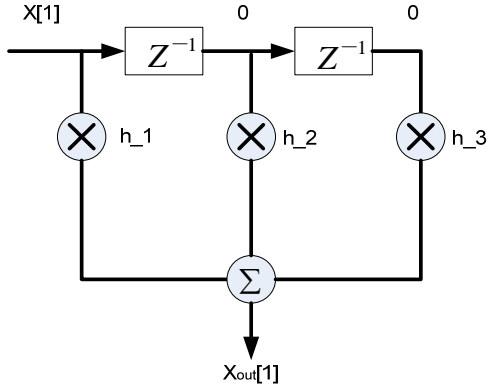
Figure2.4 X[1] passes through the multipath channel   **Figure2.5** X[n+1] passes through the multipath channel
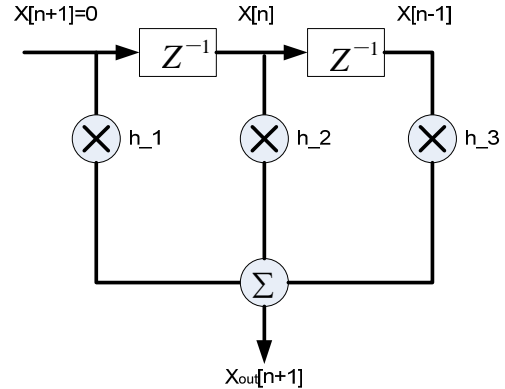
From equation 2.5, it can be observed that the two samples before $X[1]$ is 0, the output $X_{out}[1]$ is only dependent on the current input bit $X[1]$, as shown in Figure 2.2, the first output $X_{out}[1]$ after multipath lost its *cyclic property*. (In the CP-OFDM, the two samples before $X[1]$ should be $X[n]$ and $X[n-1]$, so that the *cyclic property* is maintained). Then let us consider the first ZP sample $X[n+1]$, as shown in Figure 2.2. Figure 2.5 presents the output $X_{out}[n+1]$ after multipath:

$$\begin{aligned} X_{out}[n+1] &= X[n+1] \cdot h\_1 + X[n] \cdot h\_2 + X[n-1] \cdot h\_3 \\ &= X[n] \cdot h\_2 + X[n-1] \cdot h\_3 \end{aligned}$$

$$(2.6)$$

In order to maintain the *cyclic property*, adding output $X_{out}[N+1]$ to $X_{out}[1]$ is a necessary step which is called cyclical adding, and then the new output $X_{out}^{sum}[1]$ is:

$$\begin{aligned} X_{out}^{sum}[1] &= X_{out}[1] + X_{out}[n+1] \\ &= X[1] \cdot h\_1 + X[n] \cdot h\_2 + X[n-1] \cdot h\_3 \end{aligned}$$

$$(2.7)$$

For the same principle to maintain *cyclic property*, we also need to add $X_{out}[N+2]$ to $X_{out}[2]$.

To summarize, ZP-OFDM has the lower transmission power advantage compared to CP-OFDM, the price paid is increased receiver complexity. In ZP-OFDM system, we should do the cyclical adding (add ISI part to the beginning of current OFDM symbol) to maintain the cyclic property before equalization, as shown in Figure 2.6.
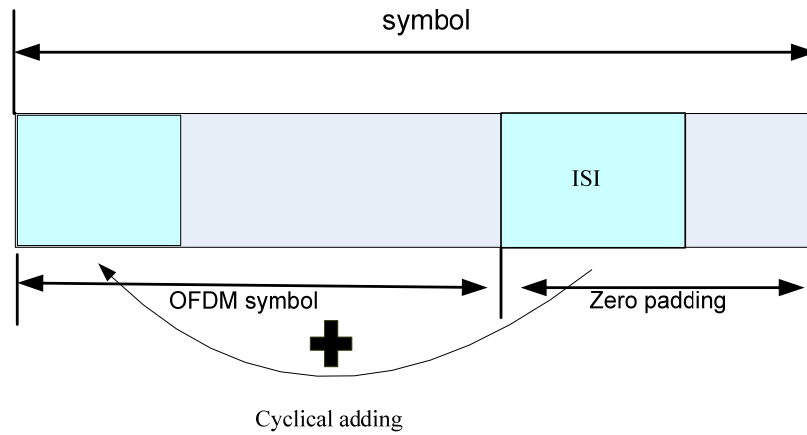
Cyclical adding

Figure2.6 cyclical adding

References

[1] John G. Proakis, "Digital Communications, 3rd Edition", McGraw-Hill Book Co., 1995

[2] Wireless Communications: Principles and Practice (2nd Edition) (Prentice Hall Communications Engineering and Emerging Technologies Series) by Theodore S. Rappaport

[3] A. Scaglione, G. B. Giannakis, and S. Barbarossa, "Redundant filterbank precoders and equalizers—Part I: Unification and optimal designs and Part II: Blind channel estimation, synchronization and direct equalization,"IEEE Trans. Signal Processing, vol. 47, pp. 1988–2022, July 1999.

Chapter 3.   MB-OFDM UWB System

In 2005, the WiMedia Alliance [1] working with the European Computer Manufacturers Association (ECMA) announced the establishment of the WiMedia MB-OFDM (Multiband Orthogonal Frequency Division Multiplexing) UWB radio platform as their global UWB standard-ECMA-368. ECMA-368 was also chosen as the physical layer (PHY) of high data rate wireless specifications for high speed Wireless USB (W-USB), Bluetooth 3.0 and Wireless High-Definition Media Interface (HDMI). Recently ECMA-368 has published a second updated version [2]. Based on the basic principles of OFDM system introduced in chapter 2, this chapter provides a brief review of ECMA-368 MB-OFDM UWB system.

3.1   Introduction to MB-OFDM UWB system

ECMA-368 specifies an UWB physical layer (PHY) for a wireless personal area network (WPAN), utilizing the unlicensed 3.1–10.6 GHz frequency band. The MB-OFDM systems consist of 14 bands with a bandwidth of 528 MHz for each band. These bands are then grouped into five band groups. The information transmitted on each 528MHz band is modulated using OFDM. OFDM distributes the data over 122 useful subcarriers with 4.125 MHz subcarrier spacing. Frequency-domain spreading, time-domain spreading, and forward error correction (FEC) coding are used to vary the data rates, supporting data rates of 53.3, 80, 106.7, 160, 200, 320, 400, and 480Mb/s.

The MB-OFDM UWB system has two modes of operation: Time Frequency Interleaved (TFI) and Fixed Frequency Interleaved (FFI). In the TFI mode, the signal hops over two or three bands within a band group. The hopping pattern is called a Time Frequency Code (TFC), and has a period of six hops. In each hop, one OFDM symbol is transmitted .For each band group, a TFC is defined. For example, a TFC for the first band group is given as {3, 2, 1, 3, 2, 1}, as shown in Figure 3.1. In the FFI mode the system does not hop and only uses one of the 528 MHz bands.
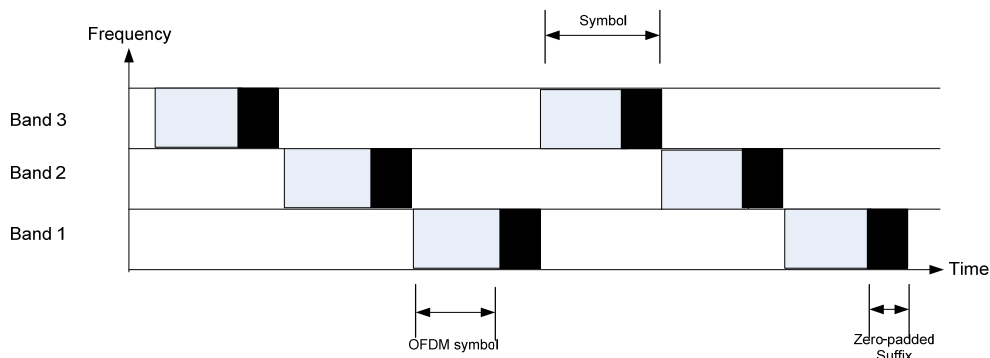
Figure3.1 Frequency hopping in the TFI mode

From Figure 3.1, it is apparent that the symbol is created by appending a zero-padded suffix (ZPS) to the OFDM symbol. As we discussed in chapter 2, the zero-padded suffix

is a common guard interval to mitigate the effects of multi-path; and it provides sufficient time for the transmitter and receiver to switch between the different central frequencies.

MB-OFDM UWB System

Figure 3.2 shows the block diagram of baseband MB-OFDM UWB system with emphasis on frequency domain processing blocks.
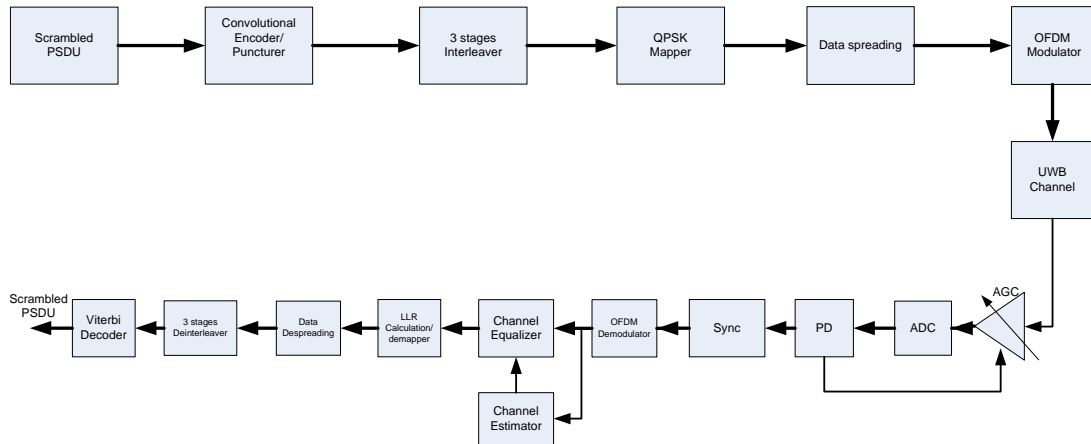
Figure3.2 Block diagram of baseband MB-OFDM UWB system

Before explaining each block in detail, we will give a brief introduction of the transmitter and receiver chain of the MB-OFDM UWB system.

Transmitter chain:
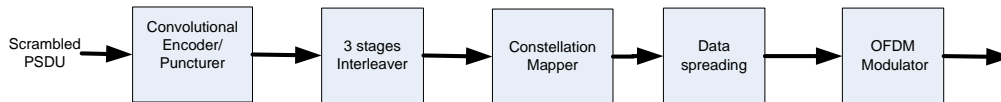
Figure3.3 Block diagram of baseband Transmitter

The transmitter is constructed according to "High rate ultra wideband PHY and PDU standard" [2]. After the scrambled PLCP Service Data Unit (PSDU) (will be discussed in Chapter 3.2) are encoded according to standard code rate 1/3, puncturer is used to control the code rate. This coded block is interleaved and spread prior to modulation in order to provide better frequency diversity. Interleaved data is then mapped onto QPSK constellation when the data rate is low (53.3, 80, 106.7, 160, 200 Mbps) or Dual Carrier Modulation (DCM) constellation when the data rate is high (320, 400, 480 Mbps) respectively [2]. After constellation mapping, the data to be sent may be spread over the frequency domain and time domain, depending on different data rates. Then, IFFT operation converts 128 sub-carrier tones which are spaced 4.125 MHz apart from each other. Finally, instead of a more traditional cyclic prefix, each symbol (including the preamble and training sequences) is padded with $N_{zp} = 37$ zeros.

Receiver chain:
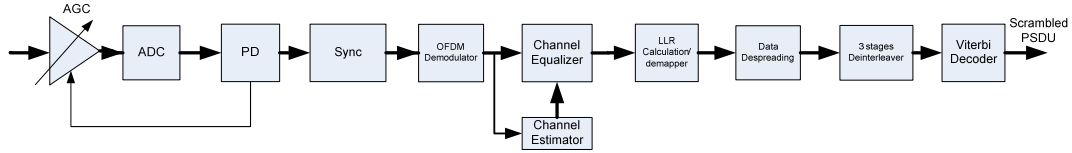
Figure3.4 Block diagram of baseband Receiver

At the receiver, first the transmitted OFDM signal passes through the Automatic Gain Control (AGC) block, which consists of Power Detection (PD) and Variable-gain Amplifier (VGA). When PD detects the signal is strong, the VGA reduces the volume effectively and when PD detects the signal is weak, VGA raises the signal. Then the continuous OFDM signal is converted to discrete digital samples through Analog-to-digital converter (ADC). After synchronization, ZPS is removed first, and then the discrete OFDM signal is converted into N frequency domain complex value through the FFT operation. Before demapping stage, an equalizer is necessary to compensate the distorted data which is caused by the fading channel drifting. After equalization, the soft information is represented by a Log-Likelihood Ratio (LLR) at the bit level. [3]. Later after data despreading, the information bits are properly demapped and deinterleaved. Finally, transmitted information bits are recovered by a Viterbi Decoder.

3.2   PSDU

The data packet on the physical layer is referred to PPDU (PLCP Protocol Data Unit). A PPDU consists of three components; the PLCP (Physical Layer Convergence Protocol) preamble, the PLCP header and the PSDU (PLCP Service Data Unit), which contains the actual information data (coming from higher layers), as shown in Figure 3.5. To transmit a PSDU, ECMA-368 has eight transmission modes by applying various levels of coding and diversity to offer 53.3, 80, 106.7, 160, 200, 320, 400 or 480Mb/s to the MAC layer. In the NBI mitigation research work, we limited ourselves to the PSDU section, which contains the information bits.
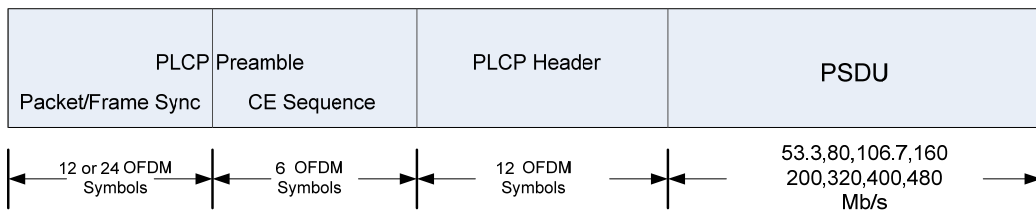
Figure3.5 PPDU structure

The PSDU is the last major component of the PPDU. The data section of the frame is subdivided into the fields Payload, FCS (Frame Check Sequence), tail and pad bits, as shown is Figure 3.6. The 6 tail bits are used to reset the convolutional coder to zero. The data field must be filled with the full number of OFDM symbols. Additional bits that may

be available are set to 0 as pad bits. Data must first be scrambled before encoded; the scrambling sequence is given by the following generator polynomial: $g(D) = 1 + D^{14} + D^{15}$
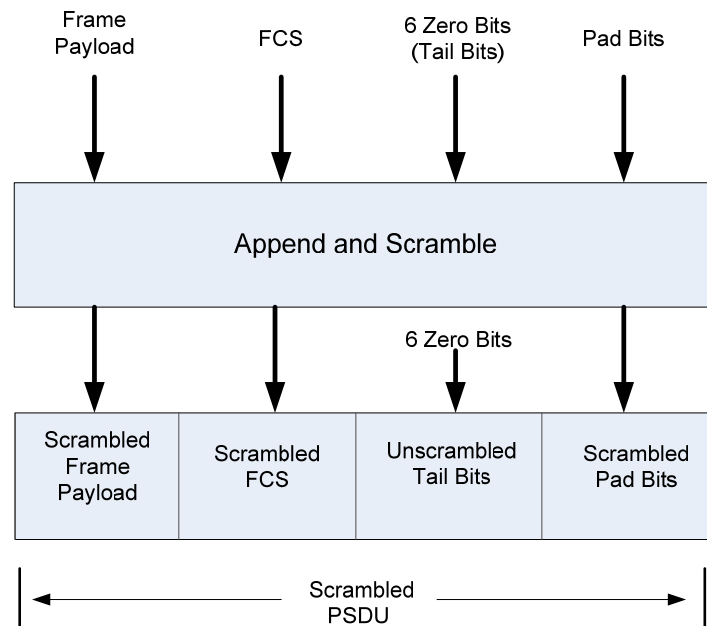
Figure3.6 Block diagram of PSDU construction [2]

3.3 Convolutional Encoder and Puncturer

In a multipath fading channel, all subcarriers have different attenuations. Some subcarriers may even be completely lost because of deep fades. Therefore, the overall PER may be largely dominated by a few subcarriers with the smallest amplitudes. To avoid this problem, channel coding can be used. By using coding, errors can be corrected up to a certain level depending on the code rate and type. A subsequent convolutional coder adds redundancies to the scrambled PSDU. The coder uses the rate R=1/3, has 64 possible states (k=7) and is described by the polynomials $g_0 = 133_8$, $g_1 = 165_8$, and $g_2 = 171_8$. To obtain the data rates of 53.3 to 480 Mbps defined by the standard, different channel code rates are required. Bits generated by the convolutional coder are therefore punctured (e.g. omitted) depending on the setting so that 1/2, 1/3, 3/4 or 5/8 code rates are attained.

3.4 Three Stages Bit Interleaver

To randomize the occurrence of bit errors, coded data are interleaved after convolutional coder. Employing frequency diversity within a band, across subcarriers and time domain spreading are three interleaver stages that ensure robustness against burst errors, as shown in Figure 3.7. The adjacent bits of the convolutional coder are first symbol interleaved, i.e. the coded and padded bit stream is distributed across 6 consecutive OFDM symbols. The second stage is the inter-symbol tone interleaving, which distributes

the bits across the data subcarrier within one OFDM symbol. Finally, the bits are cyclically shifted in successive OFDM symbols.

$$a[i] \longrightarrow \boxed{\begin{array}{c}\text{Symbol}\\\text{Interleaver}\end{array}} \xrightarrow{a_s[i]} \boxed{\begin{array}{c}\text{Tone}\\\text{Interleaver}\end{array}} \xrightarrow{a_T[i]} \boxed{\begin{array}{c}\text{Cyclic}\\\text{Shift}\end{array}} \longrightarrow b[i]$$

Figure3.7 Block diagram of three stage bit interleaver [2]

3.5   Constellation Mapper

The coded and interleaved data sequence is mapped onto a complex constellation. Depending on the data rate, the useful carriers are subjected to a QPSK or DCM modulation. For data rate between 53.3Mbps and 200Mbps, the data sequence is mapped onto a QPSK constellation. A dual-carrier modulation (DCM) is employed for data with data rates between 320Mbps and 480Mbps.

3.6   Data Spreading

Data spreading technique is an effective scheme to improve the signal to noise Ratio (SNR) performance under multipath fading channel. As we mentioned earlier, after constellation mapping the data to be sent may be spread over the frequency domain and time domain, depending on different data rates. For data rates of 53.3 and 80Mb/s, both frequency-domain and time-domain spreading techniques shall be used; For data rates of 106.7,160 and 200Mb/s, only time-domain spreading techniques shall be used; For Data Rates of 320,400 and 480Mb/s, no spreading techniques shall be used.

3.7   OFDM Modulator

After data spreading, the data sequence is sent to the OFDM modulator. A 128 point IFFT is used to generate the 122 subcarriers (12 pilot subcarriers, 110 data subcarriers and 10 guard subcarriers), the other six subcarriers are not used (null subcarrier). In all of the OFDM symbols following the PLCP preamble, 12 pilot subcarriers are used for coherent detection and to provide robustness against frequency offsets and phase noise. The 10 guard subcarriers are located on both edges of the OFDM symbol and have same value as the 5 outermost data subcarriers. In addition, the guard carriers can be used as another form of time and frequency diversity resulting in the improvement of receiver performance.

3.8   System Requirements for Packet Error Rate

The Packet Error Rate (PER) is an important performance metric for a MB-OFDM UWB system. It is used to test the performance of the receiver. PER is the ratio, in percentage of the number of PSDU not successfully received (as long as one bit of the PSDU is incorrect at the receiver side, we regard the PSDU as not successfully received) by the

receiver to the number of PSDU sent by the transmitter. In the ECMA-368 MB-OFDM UWB system, PER less than 8% is required with a PSDU of size 1024 octets.

References
[1] WiMedia Alliance http://www.wimedia.org/en/index.asp
[2] ECMA-368, "High rate ultra wideband PHY and MAC standard," December 2007.
[3] General Log-Likelihood Ratio Expression and Its Implementation Algorithm for Gray-Coded QAM Signals ,Ki Seol Kim, Kwangmin Hyun, Chang Wahn Yu, Youn Ok Park, Dongweon Yoon, and Sang Kyu Park, ETRI Journal, vol.28, no.3, June 2006, pp.291-300.

Chapter 4. Narrowband interference in MB-OFDM UWB System

According to the Federal Communications Commission (FCC) regulations [1], UWB systems must operate within the frequency 3.1-10.6GHz, and the transmitted power level should be limited to -41.3dBm/MHz. Due to the low transmission power and huge bandwidth, UWB systems will unavoidably be impacted by the narrowband interferences (NBI), which are generated by other systems. When compared to the desired wideband signal, the interference occupies a much smaller frequency bandwidth and has a higher power spectral density. In this chapter, we first discuss the NBI interferer models in the MB-OFDM UWB system and explained the principle of NBI spectrum leakage. Then, the NBI impact on MB-OFDM UWB system is analyzed. Additionally, three existing NBI cancellation /mitigation techniques for the MB-OFDM UWB system are introduced. Finally, a comprehensive comparison among these techniques is presented.

4.1 Narrowband Interference Models in MB-OFDM UWB System

Narrowband interference can be due to the transmission signals or harmonics (caused by the nonlinearity characteristic of the power amplifier) generated from other services. These signals or harmonics may occupy the same frequency band with the MB-OFDM UWB system, and hence introduce the interference to the system. In our analysis, we limit ourselves to the cases where NBI problem is due to the harmonics generated by GSM interferer and WLAN interferer. Further, we limit our investigation to two extreme cases: 2nd harmonic of GSM signal and 3rd harmonic of WLAN signal. These two cases represent the minimum/maximal bandwidth, corresponding to maximal/ minimum power spectral density (PSD) for the same signal to interference ratio (SIR)[1].

GSM Interferer

The 2nd harmonic of a GSM signal has a constant amplitude with zero mean and constant variance. In our research, we consider the GSM signal [2] operating in the 1800 MHz bands with 0.27 MHz bandwidth. As a result, the 2nd harmonic of GSM signal operates in the 3600 MHz bands with approximately 0.54 MHz bandwidth, thus may introduces the interference to UWB system that operates within the frequency 3.1-10.6 GHz.

WLAN Interferer

The 3rd harmonic of a WLAN signal has time-varying amplitude with zero mean and constant variance. IEEE 802.11 WLAN typically works in the 2.4 GHz band with 20 MHz bandwidth, so the 3rd harmonic of WLAN signal operates in the 7.2 GHz with approximately 60 MHz bandwidth. It will spread over relatively more subcarriers

---

[1] Signal to Interference ratio (SIR): the ratio between the signal energy and the interference energy.

compared to lower order harmonics (e.g. 2nd harmonic of WLAN signal) or signals with smaller bandwidth (e.g. 3rd harmonic of GSM signal).

4.2   Spectrum Leakage Phenomenon

4.2.1   Principle of Spectrum Leakage

At the receiver side of the MB-OFDM UWB system, after cyclical adding, there is an implicit time domain rectangular windowing on the incoming symbols before the FFT operation, as shown in Figure 4.1. Multiplication in the time-domain with a rectangular function is equivalent to convolution in the frequency-domain with a sinc-like function. The sinc shape has a narrow main lobe, with many side-lobes that decay slowly with the frequency difference away from the centre. Hence the NBI could be leaked to neighboring subcarriers of MB-OFDM UWB system and affect some neighboring subcarriers. An example of spectrum leakage will be shown in the next section.
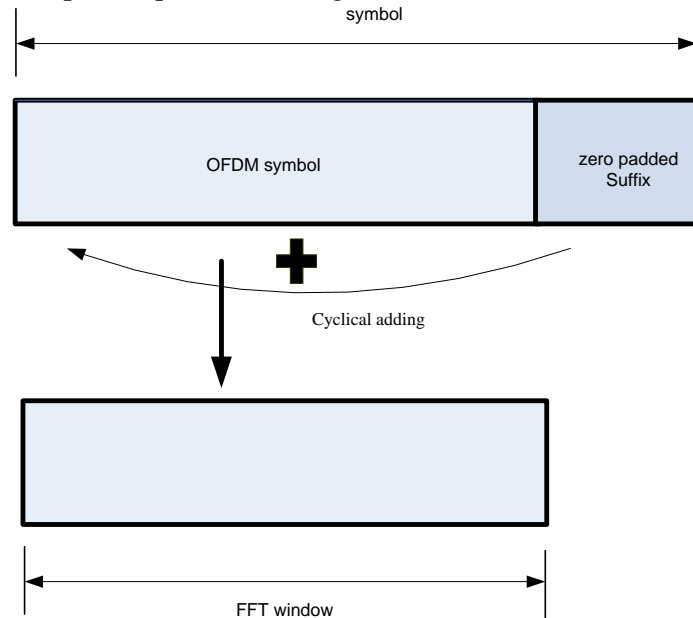
Figure4.1 FFT window on received symbol in the time domain

4.2.2   Mathematical Derivation of Spectrum Leakage

It this section, a deterministic interference model with single frequency component (shown in equation 4.1) is used to demonstrate the principle of the spectrum leakage. This interference can be regarded as a NBI with extreme small bandwidth. For NBI with large bandwidth, such as 3rd WLAN harmonic with 60 MHz, we use a second model (wide-sense stationary process) to model it, which will be discussed in chapter 5.

$$I(n) = e^{j2\pi f_c n T_s} \tag{4.1}$$

where $I(n)$ is the discrete sampling points of the time-domain interference with single frequency component f_c. n is the time index, $n = 1, 2....m$, m is the number of time-domain OFDM signal sampling points (assume one sample per bit). T_s is the sampling time.

As explained in Chapter 2, in OFDM modulation, the subcarrier frequency f_n is defined as

$$f_n = n\Delta f \qquad (4.2)$$

where

$$\Delta f = \frac{f_s}{N} = \frac{1}{NT_s} \qquad (4.3)$$

Here f_s is the entire bandwidth, and N is the number of subcarriers, suppose N=128 in this example. k is the index of the subcarrier. Suppose the interference with single frequency component f_c is located in the middle of subcarrier 81 and subcarrier 82, we get:

$$f_c = \frac{80.5}{N} f_s = \frac{80.5}{NT_s} \qquad (4.4)$$

Hence:

$$I(n) = e^{j2\pi f_c nT_s} = e^{j2\pi \frac{80.5}{N}n} \qquad (4.5)$$

After FFT we can get the frequency-domain interference samples

$$
\begin{aligned}
I(k) &= \sum_{n=0}^{N-1} I(n)e^{-j2\pi \frac{n}{N}k} = \sum_{n=0}^{N-1} e^{j2\pi \frac{f_c}{N}n} e^{-j2\pi \frac{n}{N}k} \\
&= \sum_{n=0}^{N-1} e^{j\frac{2\pi n}{N}(80.5-k)} \qquad k = 0,1,2...N-1
\end{aligned}
\qquad (4.6)
$$

$\sum_{n=0}^{N-1} e^{j\frac{2\pi n}{N}(80.5-k)}$ is a geometric series with ratio $e^{j\frac{2\pi}{N}(80.5-k)}$,

$$X_i(k) = \sum_{n=0}^{N-1} e^{j\frac{2\pi n}{N}(80.5-k)} = \frac{1-(e^{j\frac{2\pi}{N}(80.5-k)})^N}{1-e^{j\frac{2\pi}{N}(80.5-k)}} \qquad (4.7)$$

4.2.3   Simulation and Theoretical Results:

The spectrum of monochromatic interference (simulation is based on eight-times oversampling rate, simulation configuration is shows in Table 4.1, power is normalized) and normalized theoretical value (using equation 4.7, N=128) are plotted in Figure 4.2. The normalized theoretical value shows the frequency-domain interference samples on each subcarrier bin, it can be observed that the monochromatic interference is leaked to the neighboring subcarriers. The oversampled simulation presents the spectrum more

clearly, it also shows the frequency-domain samples between two adjacent subcarrier bins. The wiggles present a sinc-like shape which is caused by the fourier transform of rectangular windowing.
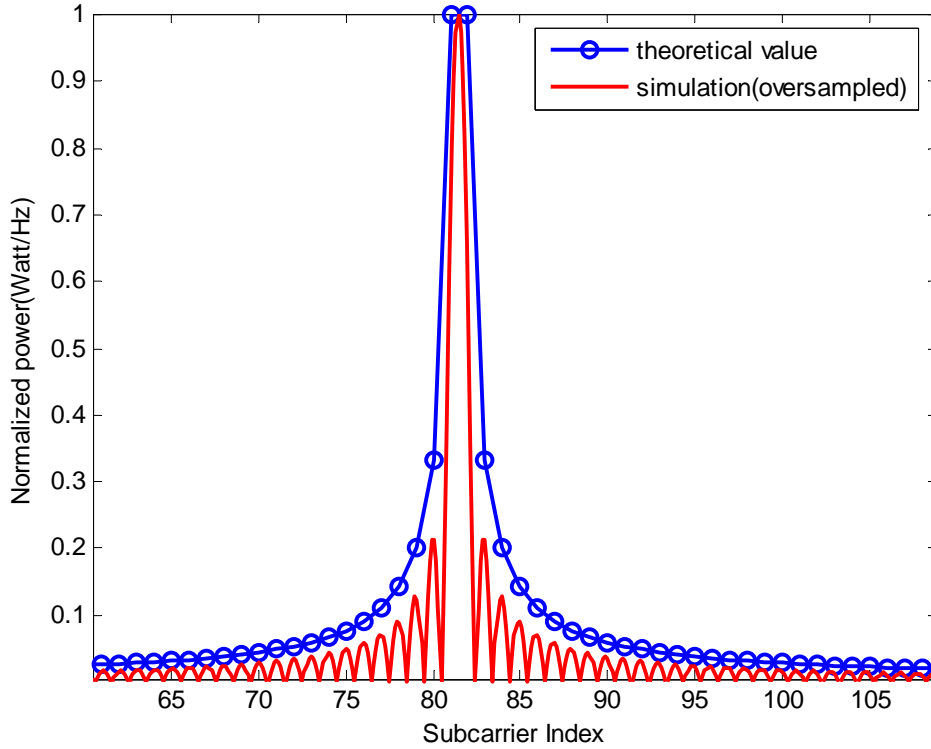
Figure4.2 Interference spectrum leakage

Number of subcarriers	N=128
Interference model	$I(n) = e^{j2\pi f_c nT_s}$
Interference frequency	Interference is located between subcarrier 81 and 82

Table 4.1 Simulation Configuration of MB-OFDM UWB System

4.3   Spectrum Leakage of Different NBI Models

In section 4.1, we briefly discussed the influence of two extreme NBI interferers with minimum/maximal bandwidth. In this section, we will investigate the relationship between spectrum leakage and NBI bandwidth in detail. Additionally, we will also research on the spectrum leakage with different NBI frequencies.

As mentioned in chapter 3, the subcarrier spacing of MB-OFDM UWB system is 4.125 MHz. For the 2nd harmonic GSM interference with approximately 0.54 MHz bandwidth, the bandwidth is relatively small compared to subcarrier spacing. In this situation, the interference location largely determines the degree of spectrum leakage influence. We

will first simulate the 2nd harmonic GSM interference at four positions between two subcarriers 31 and 32, as shown in Figure 4.3, "bin" "left", "middle" and "right" refer to the subcarrier bin frequency, one quarter ,half and three quarters of the subcarrier spacing. The simulation computes the PSD of the 2nd harmonic GSM interference (using hamming wndow) at these four positions with the same energy.
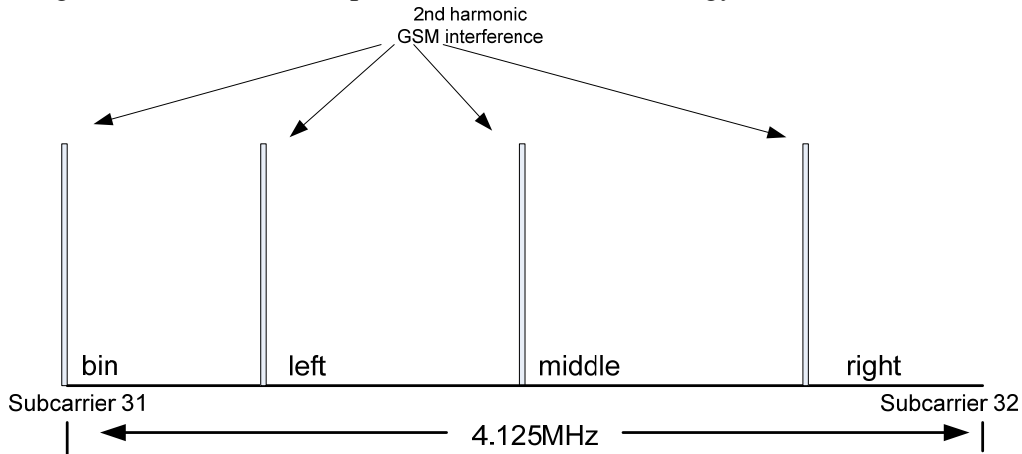
Figure4.3 GSM interference is located at four positions

Figure 4.4 shows the PSD of 2nd harmonic GSM interference with same energy located at the four positions. When GSM interference is located at subcarrier 31 bin frequencies, the system is in the first-degree spectrum leakage situation. The main GSM interference energy (99.98% of the total NBI energy) concentrates on subcarrier 30, 31 and 32, only these three subcarriers are seriously affected by the GSM interference. When GSM interference is in the middle of subcarrier bins, spectrum leakage phenomenon is most serious. The main GSM interference energy (99.98% of the total NBI energy) concentrates on approximately 40 subcarriers, from subcarrier 11 to 50, as shown in Figure 4.4. When GSM interference is located at other positions, such as "left" and "right", the spectrum leakage level will between the two extreme cases (at bin frequency and in the middle of two adjacent subcarriers).
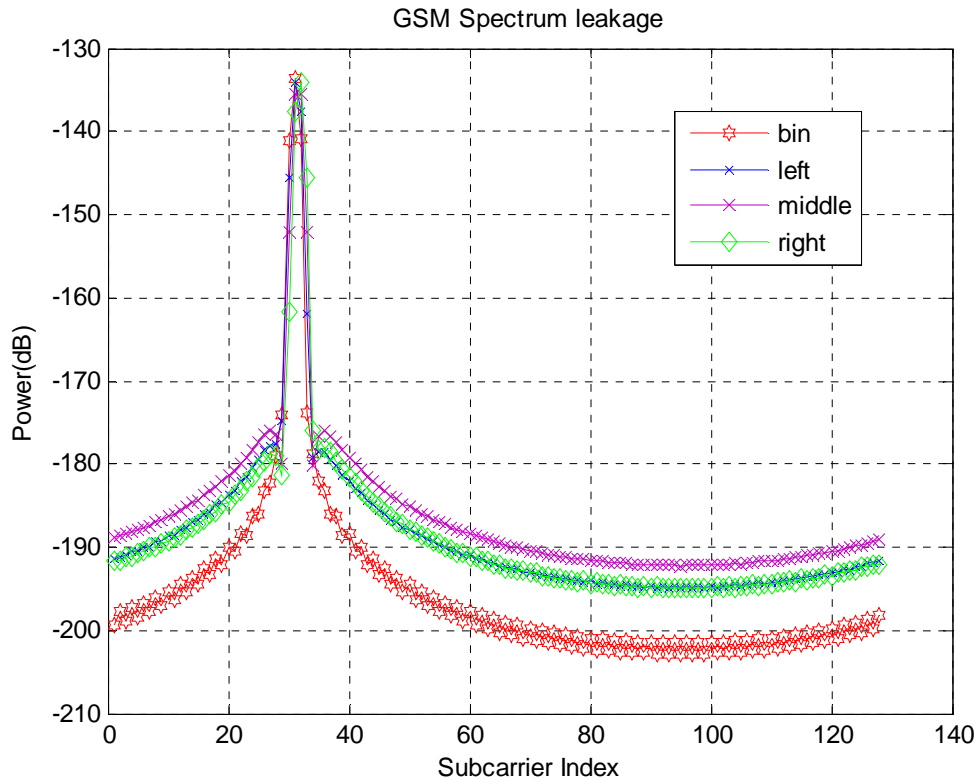
Figure4.4 GSM interference is located at four positions

Similarly, we locate the 3rd harmonic of WLAN interference at the four positions ("bin", "left", "middle" and "right") between two subcarriers 31 and 32, and then simulate the PSD of the WLAN interference (using hamming wndow) at these four positions with the same energy, as shown in Figure 4.5. As we mentioned in section 4.1, the bandwidth of 3rd harmonic interference is approximately 60 MHz, which covers about 15 subcarriers of MB-OFDM UWB system. Hence the 3rd harmonic of WLAN interference spread over relatively more subcarriers compared to 2nd harmonic GSM interference. An interesting phenomenon is found, the PSD shapes of WLAN interference at different positions are almost the same. The WLAN interference locations have little influence on the PSD shapes, which is different than the PSD of GSM at different positions shown in Figure 4.5. This is because when NBI bandwidth is larger than the subcarrier spacing, the interference contains the same frequency components at any positions.
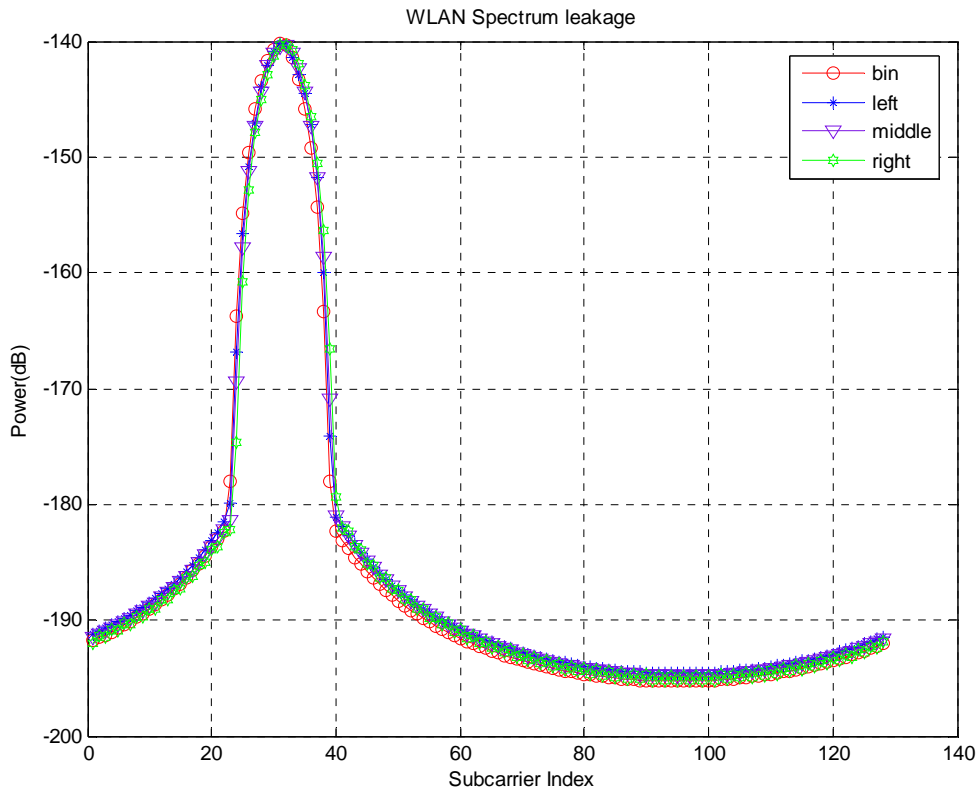
Figure4.5 WLAN interference is located at four positions

For example, suppose we consider a NBI with 4.125MHz bandwidth (equal to the subcarrier spacing of the MB-OFDM UWB system), as shown in Figure 4.6. We locate the NBI at the subcarrier bin and the midpoint between two adjacent subcarriers, in Figure 4.6 it is observed that these two cases share the same frequency components part B, actually part A and part C cover the same frequency components (the first half of the subcarrier spacing), the frequency shift between part A and C does not change the PSD shape. That is why the PSD shapes of WLAN interference remain the same at different positions. To summarize, NBI with larger bandwidth will affect relatively more subcarriers in the OFDM system than NBI with smaller bandwidth. Also the influence of NBI frequency on its PSD shape becomes less when NBI bandwidth increases.
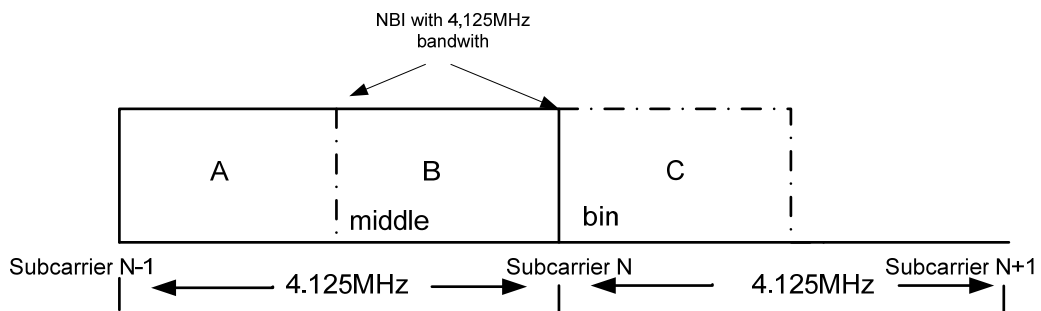
Figure4.6 NBI with 4.125M bandwidth

4.4 Impact of Narrowband Interference on OFDM UWB Receiver

After discussing the NBI Models and spectrum leakage phenomenon in previous sections, in this section we focus on the impacts of NBI on the receiver side of MB-OFDM UWB system. As we mentioned in chapter 1, the NBI is generated by the transmission signals or harmonics from other wireless systems sharing the same frequency band, as shown in Figure 4.7. The combined signal (OFDM signal combined with NBI) first passes through the low-noise amplifier (LNA) and down-converter to the baseband. Then the combined signal goes through the Automatic gain control (AGC), in order to adjust the signal volume suitable for Analog-to-digital converter (ADC). After synchronization, the discrete combined signal is converted into N frequency domain complex values through the OFDM demodulator. At the receiver side of MB-OFDM UWB system, ADC and OFDM demodulator are affected by NBI.
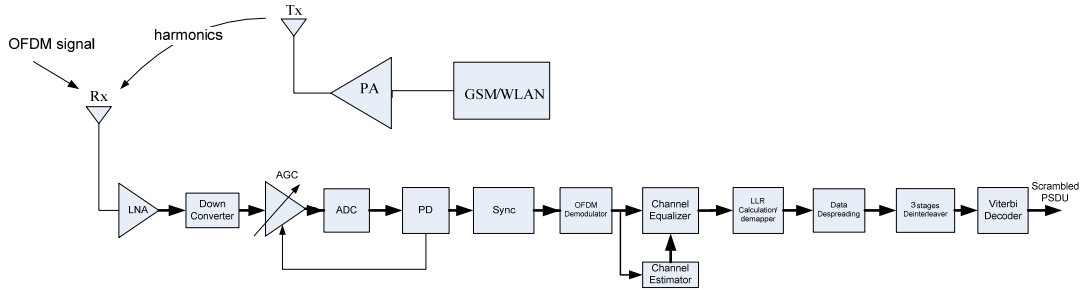
Figure4.7 Receiver of the MB-OFDM system is affected by NBI

4.4.1 NBI Impact on ADC

Suppose the full scale voltage range of ADC in our system is from -V to +V volts, and the signal level range of clean OFDM signal is from -V to +V volts. When a clean OFDM signal passes through the AGC, the signal level range does not change. The scale factor of the AGC is 1 in this case, as shown in Figure 4.8. The ratio between OFDM signal amplitude and ADC quantization noise is equal to $\dfrac{V-(-V)}{\Delta Q}=\dfrac{2V}{\Delta Q}$, where ΔQ is the ADC quantization noise.
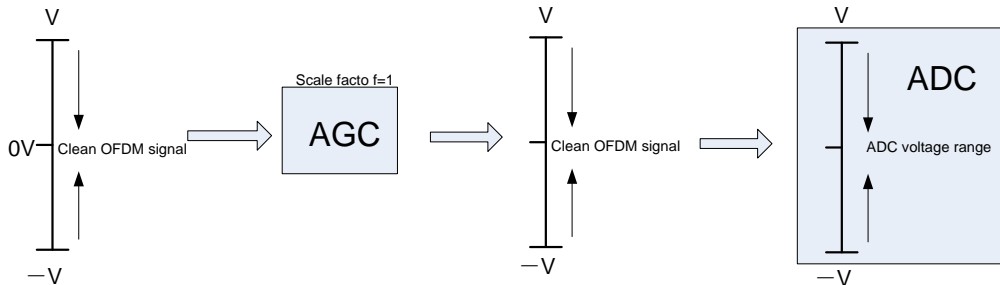
Figure4.8 Clean OFDM signal passes through ADC

Figure 4.9 shows the case when clean OFDM signal is influenced by NBI, the signal level range of combined signal (OFDM signal plus NBI) is from -aV to +aV volts, where a is scalar constant (a>1). In order to satisfy the full scale voltage range of ADC, the

combined signal has to scale down after AGC, the scale factor is 1/a, as shown in Figure 4.9. After AGC the clean OFDM signal only occupy 1/a proportion of the combined signal, hence the ratio between OFDM signal amplitude and ADC quantization noise is equal to $\dfrac{\frac{V}{a}-(-\frac{V}{a})}{\Delta Q}=\dfrac{\frac{2V}{a}}{\Delta Q}$. It can be concluded that NBI will decrease the ratio between OFDM signal amplitude and ADC quantization noise, thus resulting in the lower accuracy on the following blocks after ADC at the receiver side.
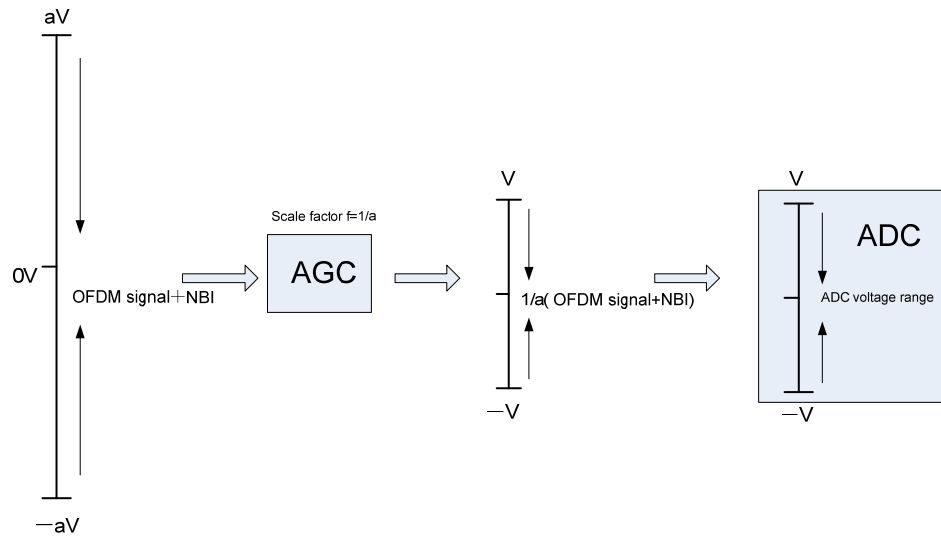
Figure4.9 OFDM signal with NBI passes through ADC

4.4.2 OFDM Demodulator:

The NBI spectral leakage phenomenon in the MB-OFDM system was explained in previous sections. From Figure 4.4 and 4.5, it can be observed that the OFDM signal on the center subcarrier (where the NBI interference is located) and its adjacent subcarriers are corrupted by NBI due to the spectral leakage. During the demodulation, those corrupted subcarriers will degrade the system PER performance of MB-OFDM UWB receiver.

4.5   Current Narrowband Interference Mitigation Techniques

ECMA-368 High Rate Ultra Wideband PHY and MAC Standard [4] specifies the transmitter side of the MB-OFDM UWB system, so the potential NBI cancellation/ mitigation approaches only can be implemented on the receiver side. In the following we will introduce three existing NBI cancellation/mitigation techniques, which are applied to the receiver side of MB-OFDM UWB system.

Before starting this section, we first introduce two definitions. (1) Interference power level threshold: A certain power level; (2) seriously corrupted subcarrier: When the NBI

power on one subcarrier is larger than the interference power level threshold, this subcarrier is called seriously corrupted subcarrier.

4.5.1 Tone Nulling

Tone nulling is an operation at the receiver side of OFDM system after FFT. It involves finding the seriously corrupted subcarriers and erasing the information on these subcarriers: through power detection, those seriously corrupted subcarriers are found first. Then the tone nulling technique simply sets the magnitude of those seriously corrupted subcarriers to zero. The lost information of these subcarriers can be compensated by channel coding and bit interleaving techniques. Tone nulling can significantly improve the PER performance, because the MB-OFDM UWB system discards the seriously corrupted subcarriers at the OFDM demodulator in which the OFDM signal is polluted by NBI.

Let us take an example to illustrate tone nulling technique. We simulate the PSD of OFDM signal and 3rd harmonic of WLAN interference in the MB-OFDM UWB system, using the simulation configuration in Table 4.2. The simulation result and interference power level threshold (the threshold setting depends on the system accuracy requirement) are shown in Figure 4.10. We can see the 3rd harmonic of WLAN interference will seriously affect approximately 15 subcarriers in the MB-OFDM UWB systems. When using tone nulling technique, we should erase the information on these 15 subcarriers.

OFDM-base system type	MB-OFDM UWB system
Bandwidth of system	528MHz
Number of subcarriers	N=128
Number of Zero padding	$N_{zp} = 37$
Size of FFT window	$N_{FFT} = 128$
NBI model	3rd harmonic of WLAN interference with 60MHZ bandwidth
SIR	-20dB
OFDM signal power	-54.7dBm/MHz

Table 4.2 Simulation Configuration
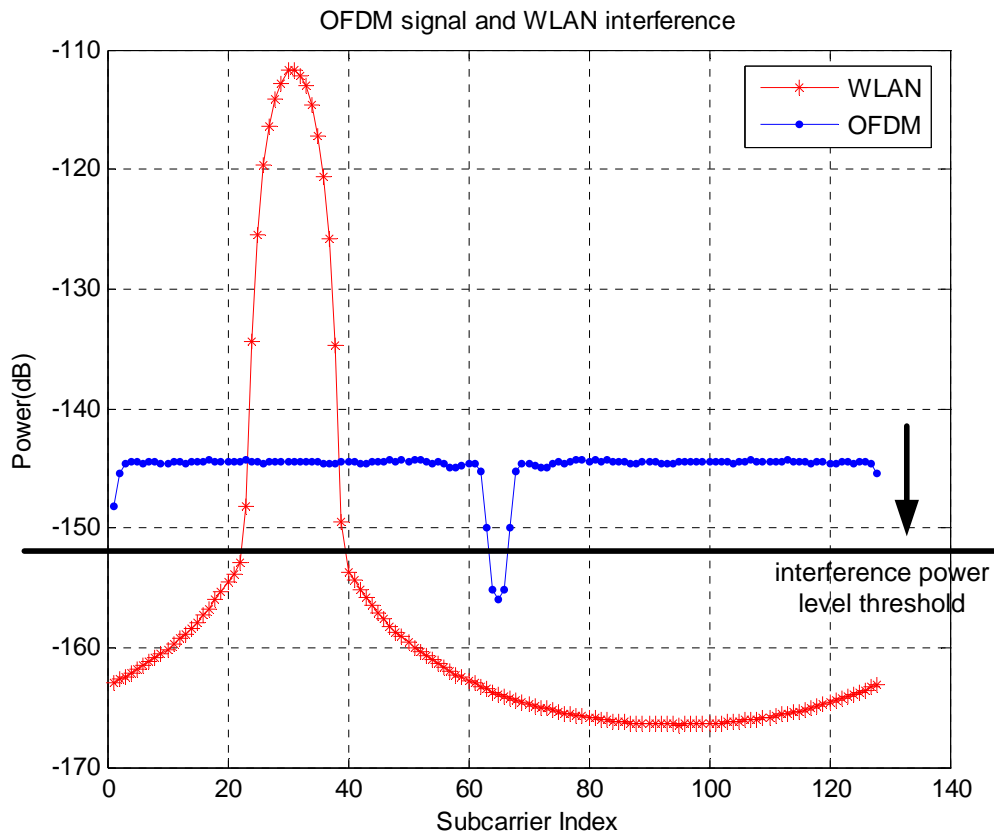
Figure4.10 Spectrum of OFDM signal and WLAN

Tone nulling can mitigate the NBI impact on the OFDM demodulator and is easy to implement, however it has some limitations: (1) It doesn't mitigate the NBI impact on ADC; (2) When the system suffers from strong NBI, tone nulling can not reduce the large signal level range of combined signal (OFDM plus NBI) before it enters into the OFDM demodulator. From the hardware design point of view, the OFDM demodulator will need more bits to represent the signal with large signal level range.(3) OFDM signal information on those corrupted subcarriers is lost due to tone nulling and hence reduces the PER performance.

4.5.2   Notch Filter

Notch filter is a band-stop filter with a narrow stop-band. After the NBI frequency and bandwidth are estimated in the frequency domain, we can add a notch filter based on the estimation in the time domain (before the ADC). By applying a notch filter, the NBI energy is reduced before it enters the OFDM demodulator. Hence less NBI energy will spread over on the MB-OFDM UWB spectrum after FFT.

Essentially, the principles of tone nulling and notch filter are the same; in the following we discuss the small differences between them. Tone nulling is applied in the frequency domain and erases the NBI influence on those seriously corrupted subcarriers completely.

However the other subcarriers are still affected by the NBI spectrum leakage, although the impact of NBI becomes weak when the subcarrier is far from center subcarrier (where the NBI is located). Notch filter is applied in the time domain and reduces the NBI energy before FFT. As a result, in the MB-OFDM UWB spectrum, all the subcarriers are much less affected by NBI (compared without notch filter).

A notch filter can reduce the NBI energy largely before NBI spread over the MB-OFDM UWB spectrum; this operation can mitigate the NBI impact on both the ADC and OFDM demodulator. The limitations of notch filter are: (1) It is based on accurate estimation of NBI central frequency and bandwidth, which is limited under multi-interferer sources; (2) Compared with tone nulling, notch filter can reduce the large signal level of the combined signal (OFDM plus NBI) before it enters into the OFDM demodulator, hence the OFDM demodulator need less bits to represent the mixed signal (3) In [3], the difficulty in the notch filter design was mentioned. On the one hand, the notch filter should provide sufficient notch bandwidth to allow for estimation errors and time variation in the NBI; on the other hand, it also needs to restrict notch bandwidth to minimize the impact of the notch filter on data bearing subcarriers which are less affected by NBI; (4) Notch filter need to be redesigned if the NBI sources change or relocated if the NBI frequency changes.

4.5.3 Windowing Technique

Receiver windowing is a technique [5, 6] that can be applied to OFDM systems. However, current receiver windowing techniques are only available for CP-OFDM scheme. In this section, we will introduce the principle of receiver windowing. Based on this principle, we try to design a new receiver windowing for ZP-OFDM scheme, which will be presented in chapter 5. The main steps for receiver windowing operation for CP-OFDM system is shown in Figure 4.11.
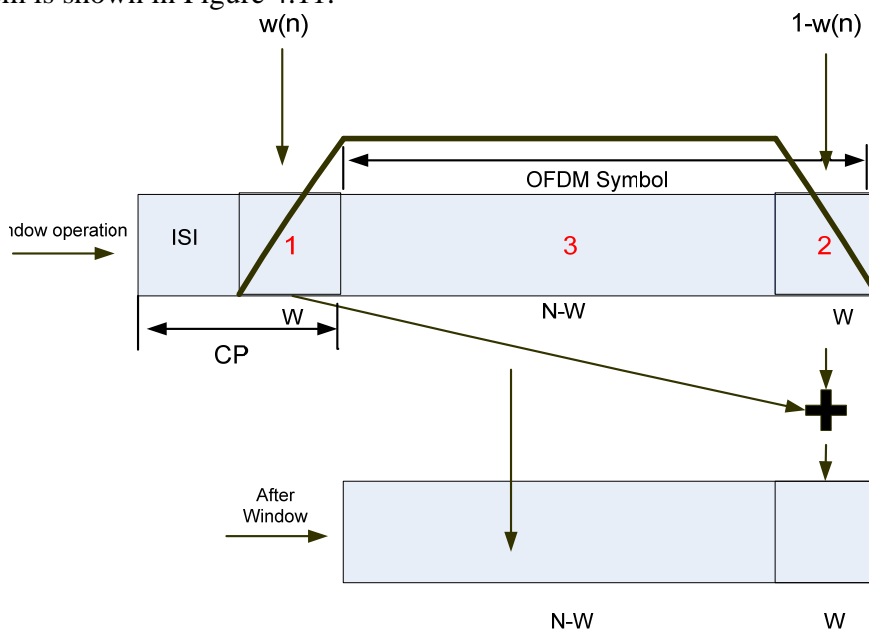
Figure4.11 Receiver windowing for CP-OFDM system

where CP refers to the cyclic prefix, ISI (inter symbol interference) refers to CP samples which are affected by multipath. The marked numbers refer to three parts of one symbol: Part 1 refers to the W clean samples of CP, which aren't affected by multipath; Part 2 refers to the last W samples of one OFDM symbol; Part 3 refers to the rest N-W samples of one OFDM symbol. $w(n)$ is the window coefficients ,n=1,2,3….W. Receiver windowing multiplies the last W samples of CP by the window coefficients $w(n)$, n=1, 2…W and adds them to the last W samples of the received OFDM symbol multiplied by $1 - w(n)$ (see Figure 4.11). The last N samples of the windowed block are then sent to the FFT. The windowing operation can be viewed as a mapping from N+W to N samples through a window in Figure 4.11. Receiver windowing uses samples from the CP to construct a window which affects the NBI components without changing the data components, and meanwhile the receiver FFT size can be retained. Hence the NBI is convolved with a window which has lower side lobes than the sinc function in frequency domain, which limits the spreading of NBI to neighboring subcarriers.

Receiver windowing is easy to implement and only needs simple preprocessing prior to the FFT operation without changing the FFT size. Also receiver windowing does not need to estimate the central frequency and bandwidth of NBI, so it can work even under multi-interferer sources. Another advantage of the receiver windowing is that it does not need be redesigned when the NBI changes. Also receiver windowing has limitations: (1) The aim of receiver windowing is to lower side lobes of the NBI in the frequency domain rather than reduce the NBI energy as the previous two techniques, so the SIR gain of receiver windowing is smaller when compared to the other three techniques. (2) The length of the receiver windowing W is limited by the clean samples in the Guard interval (CP or ZPS), depending on the multipath condition.

4.6   Conclusion

In this chapter, three existing NBI cancellation/mitigation techniques were presented. Here we can classify them into two categories:

The first category can be called *NBI cancellation approaches*. Tone nulling and notch filter belong to this category. This kind of approaches aims to cancel the NBI energy as much as possible, which can be done either in time domain or frequency domain. The other category can be called *NBI mitigation approaches*. Receiver windowing techniques belong to this category. This kind of approaches uses extended window function in OFDM receiver to lower side lobes (compared to sinc function) of the NBI in frequency domain, thus can suppress the NBI energy on neighboring subcarriers. The window techniques do not need to estimate the NBI central frequency and bandwidth, and can take effect even under multi-interferer sources.Another advantage of receiver windowing is that it does not need to be redesigned when the NBI interferer changes. However, the achievable windowing gains are not tremendous as NBI cancellation approaches, because the principle of receiver windowing is to lower side lobes of the NBI in the frequency rather than reduce the NBI energy (the principle of the first category).

Based on the comparison and analysis of the three existing NBI cancellation/mitigation techniques above, we try to design a mixed scheme that consists of NBI cancellation approaches and receiver windowing, which combines the merits from both techniques. On one hand, the NBI energy on its main lobe can be largely reduced by NBI cancellation techniques. On the other hand, the receiver windowing can suppress the NBI spectrum leakage on the sidelobes, which compensates the SIR degradation caused by estimation errors effect (refer to the errors in NBI central frequency and bandwidth estimation) on the NBI cancellation approaches, also the receiver windowing does not need to be redesigned when the NBI changes. In the simulation, receiver windowing combined with tone nulling (due to its easy implementation) is chosen as the mixed scheme, as shown in Figure 4.12. In the analysis, we do not take into account the increase for the signal level range of the signal and its influence on the synchronization block of the receiver.

Figure4.12 mixed NBI cancellation scheme

In the mixed NBI cancellation scheme, the existing tone nulling techniques does not need any change. However, as we mentioned in section 4.5.3, all the existing receiver windowing are designed for CP-OFDM scheme, which cannot be applied to ECMA-368 MB-OFDM UWB system. Therefore, in Chapter 5 the work will focus on the receiver windowing design for ZP- OFDM scheme.

References

[1] Federal Communications Commission, New public safety applications and broadband Internet access among uses envisioned by FCC authorization of ultra-wideband technology Feb. 2002 [Online]. http://www.fcc.gov

[2] 3GPP TS 45.004 V6.0.0 (2005-01) 3rd Generation Partnership Project; Technical Specification Group GSM/EDGE Radio Access Network; Modulation (Release 6)

[3] "Impacts of Narrowband Interference on OFDM-UWB Receivers: Analysis and Mitigation Kai Shi; Yi Zhou; Kelleci, B.; Fischer, T.W.; Serpedin, E.; Karsilayan, A.I.; Signal Processing, IEEE Transactions on Volume 55, Issue 3, March 2007 Page(s):1118 – 1128

[4] "Standard ECMA-368 High Rate Ultra Wideband PHY and MAC Standard", 2nd Edition - Dec 2007

[5] "Receiver Window Design for Muiticarrier Communication Systems", A. J. Redfern, IEEE Journal Selected Areas in Communications, vol. 20, no. 5, pp. 1029-1036, June 2002.

[6] Optimum Nyquist windowing for improved OFDM receivers Muller-Weinfurtner, S.H.; Huber, J.B.; Global Telecommunications Conference, 2000. GLOBECOM '00. IEEE Volume 2, 27 Nov.-1 Dec. 2000 Page(s):711 - 715 vol.2 Digital Object Identifier 10.1109/GLOCOM.2000.891232

Chapter 5.   Receiver Windowing Design

In the OFDM based UWB systems, ZP-OFDM transmission becomes an appealing alternative to the traditional CP-OFDM due to its lower transmission power. In this chapter, the windowing design objectives are discussed first. Then the traditional rectangular windowing and three testing windowing schemes for ZP-OFDM system are analyzed. Base on the comparison among different windowing schemes, a new windowing shape is proposed finally.

5.1   Windowing Design Objectives

The main working principle of receiver windowing is to concentrate NBI energy on its main lobe and lower the sidelobes of its spectrum. Implementing an extended and smooth window (compared to traditional rectangular window) can suppress the NBI energy leakage to its sidelobes, however it is not necessary to add the receiver windowing in every condition. Whether using windowing or not depends on different SIR levels in the system. Figure 5.1 and Figure 5.2 show the spectrum of 3rd WLAN harmonic and ZP-OFDM symbol (using hamming window) under two extreme SIR levels, the simulation configurations are shown in Table 5.1, respectively.

Number of subcarriers	N=128
Interference model	3rd WLAN harmonic
WLAN frequency	Interference is located between subcarrier 81 and 82
SIR(dB)	-30dB and -10dB

Table 5.1 Simulation Configurations

Strong NBI environment

Figure 5.1 shows the spectrum in the strong NBI environment (SIR=-30dB), the maximal power difference between OFDM signal and WLAN harmonic is approximately 10dB, hence the OFDM signal is influenced by the 3rd WLAN harmonic in each subcarrier. In strong NBI environment, tone nulling can be used to cancel the NBI energy on its main lobe, and receiver windowing can be applied to minimize NBI sidelobes.

Weak NBI environment

Figure 5.2 shows the spectrum in the weak NBI environment (SIR=10dB). It can be observed from the plot, only the OFDM signal on the central subcarrier or neighboring subcarriers is obviously affected by WLAN interference. For other subcarriers, the power difference between OFDM signal and WLAN harmonic is larger than 30dB, the interference on those subcarriers is so weak that can not influence the OFDM signal. As a result, in the weak NBI environment only tone nulling is needed to cancel the main lobe

NBI energy. Although receiver windowing can still lower the sidelobes of NBI spectrum, actually it doesn't change the PER performance obviously.
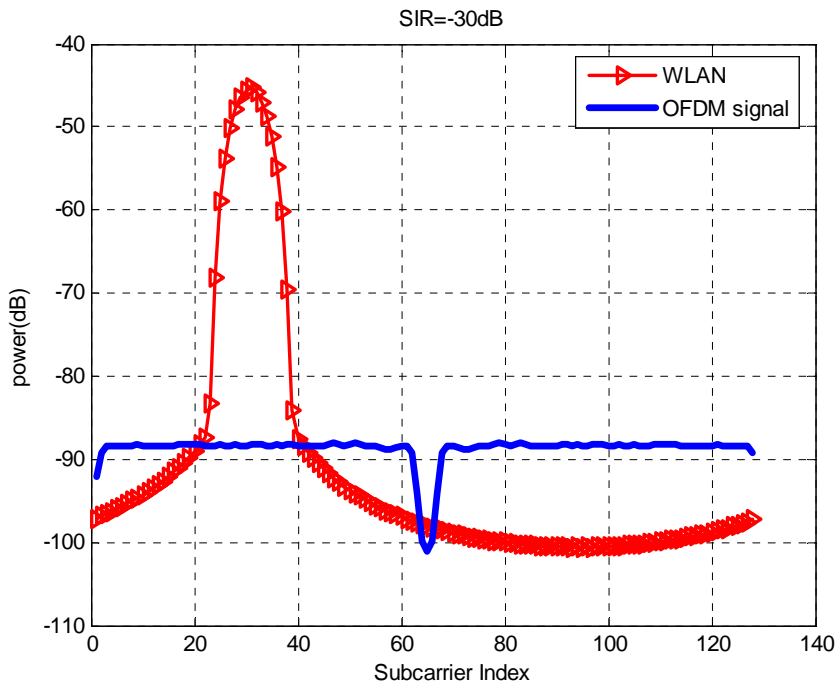
Figure5.1 Strong NBI environment
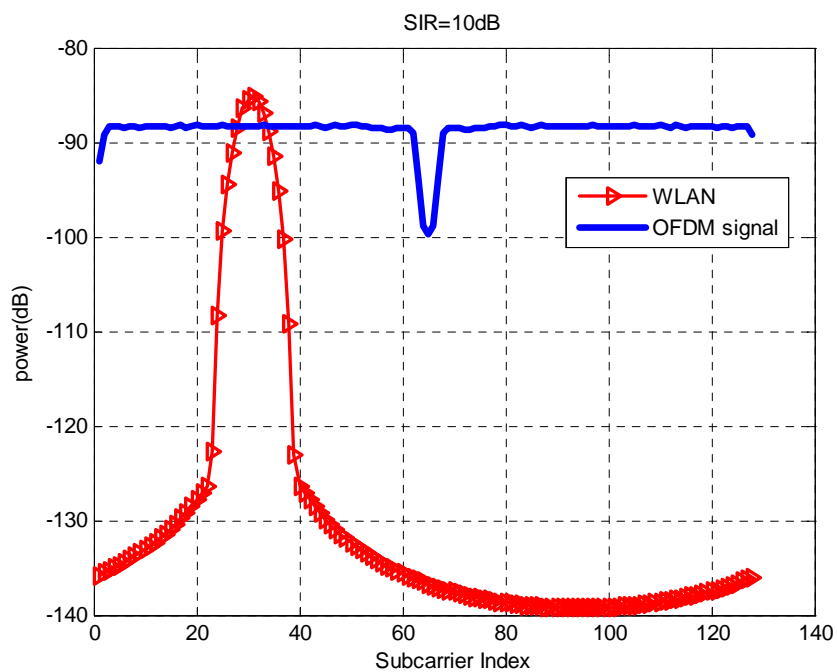
Figure5.2 Weak NBI environment

5.2   Traditional Receiver Windowing for ZP-OFDM

As introduced in section 3.1, ZPS is removed before FFT operation at the receiver side of ZP-OFDM system. It is equal to an implicit time domain rectangular window added on the incoming OFDM symbol, as shown in Figure 5.3. The cyclical adding is a necessary step before ZPS removal, this summation step maintains the *cyclic property* of ZP-OFDM symbol (discussed in section 2.6). After the summation step, one-order frequency domain equalization can still be implemented in the ZP-OFDM system as CP-OFDM. This summation step is required before windowing operation in our ZP-OFDM system, hence in the following receiver windowing design, we don't mention this step in particular.
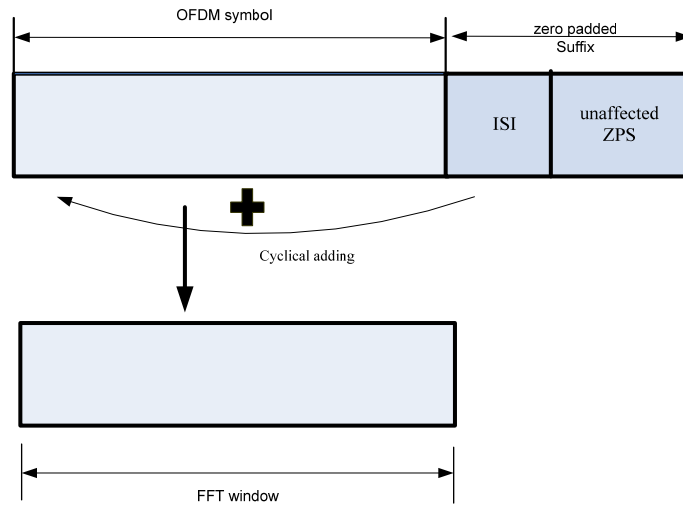
Figure5.3 Traditional receiver windowing for zero-padded OFDM

5.3   Three Testing Windowing Schemes

In this section, three testing windowing schemes will be presented for ZP-OFDM system. Before introducing the working principle of three windowing schemes, let us first investigate the impact of NBI and AWGN on the OFDM signal from the time domain point of view. At the receiver side of system, the received OFDM signal is:

$$r(t) = s(t) \otimes h(t) + nbi(t) + noise(t) \qquad (5.1)$$

where $s(t)$ is the transmitted OFDM signal, $r(t)$ is the received OFDM signal, $\otimes$ is the convolution operation, $h(t)$ is the channel impulse response, $nbi(t)$ is time domain NBI signal, $noise(t)$ is time domain additive white Gaussian noise.

When we have a noise and NBI free environment, at receiver side, the unpolluted OFDM signal is:

$$r_{clean}(t) = s(t) \otimes h(t) \qquad (5.2)$$

Define the error $e(t)$ between the received OFDM signal and unpolluted OFDM signal as follows:

$$e(t) = r(t) - r_{clean}(t) \qquad (5.3)$$

From equation 5.3 it can be observed that, in order to improve PER performance, error $e(t)$ should be minimized .In other words, the objective is to minimize the impact of NBI and AWGN, and meanwhile maintain the unpolluted OFDM signal. Then the three testing windowing schemes are presented as follows:

Testing Windowing Scheme1

Testing windowing scheme1 is shown in Figure 5.4, the number marked parts: part1, 2 refer to 2 same-shaped triangles respectively. h is the triangle height, h=1. N is the triangle width, in this example 16 samples are used from previous ZP and current ZP respectively to construct the windowing. $w(n)$ and $1-w(n)$ are the window coefficients in part1 and part2 respectively, $n = 1, 2, ...N$ .After cyclical adding, three steps receiver windowing operations are shown in Figure 5.4:
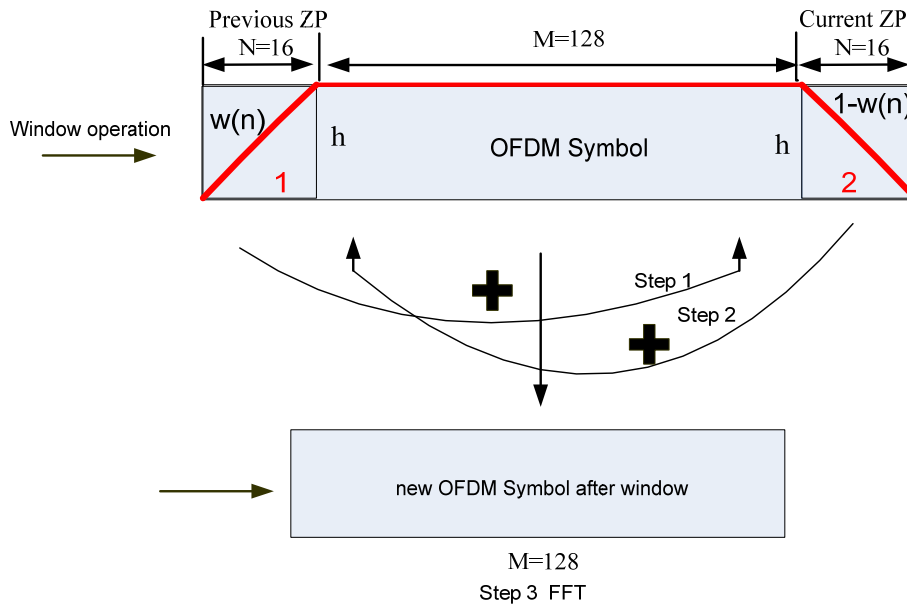
Figure5.4 Testing windowing scheme1

Step1: Multiplying the N samples of part1 by the window coefficients $w(n)$, and adding them to the end of OFDM symbol, $n = 1, 2, ...N$.

Step2: Multiplying the N samples of part2 by the window coefficients $1 - w(n)$, and adding them to the beginning of OFDM symbol, $n = 1, 2, ...N$.

Step3: ZP is removed first, and then the new OFDM symbol is sent to FFT block.

In the testing windowing scheme1, OFDM signal is maintained without any corruption., and meanwhile the traditional rectangular window is modified by a extended windowing with lower sidelobs. The triangular shape in Figure5.4 can be replaced by other smooth windowing shape, such as constant and hamming (raised-cosine window) etc, as shown in Figure 5.5, the corresponding spectrums for different windowing shapes are presented in Figure 5.6.
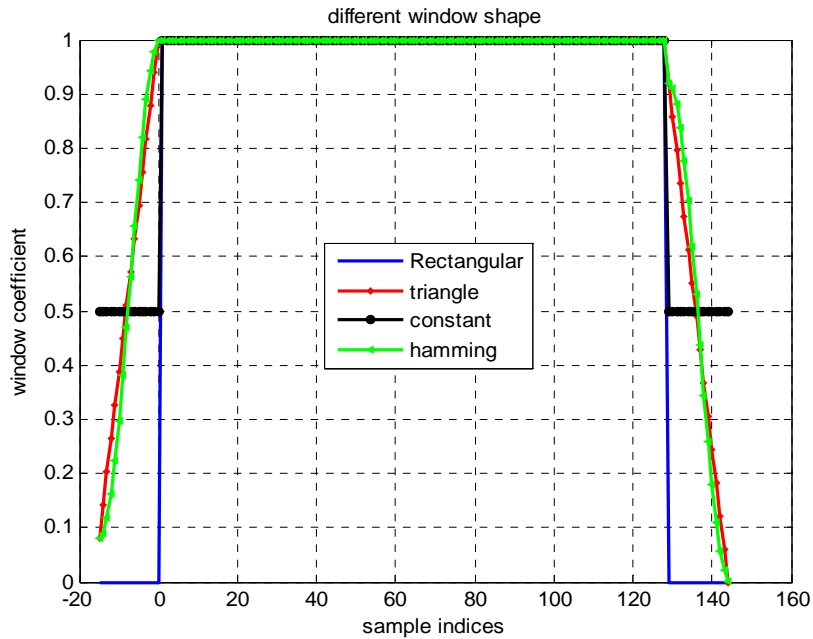
Figure5.5 Different windowing shapes for scheme1
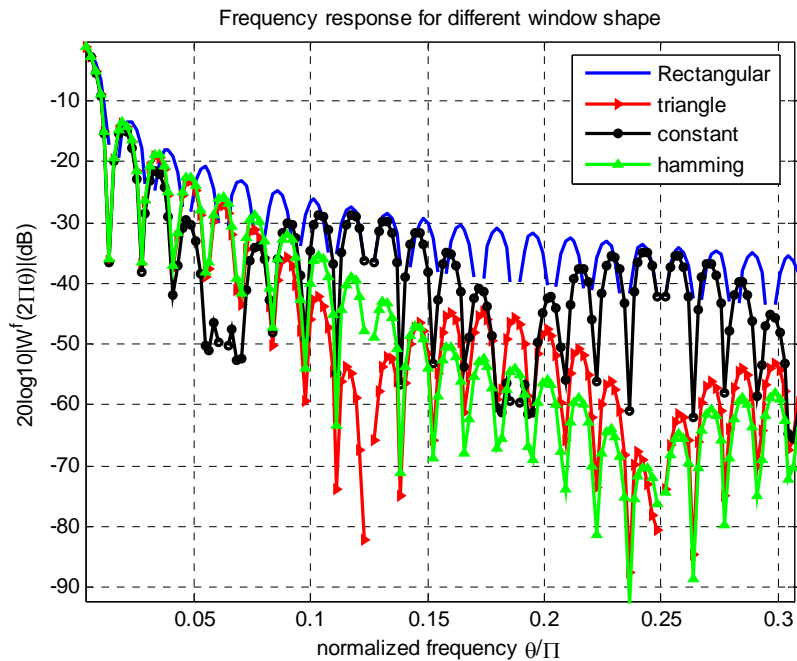
Figure5.6 Different windowing spectrums for scheme1

From Figure 5.6 it can be observed, the sidelobes of triangular and hamming windows are much smaller when compared to rectangular windowing, consequently these windowing shapes can suppress the NBI leakage. However, this scheme has its limitations: it can increase the NBI power during step1 and step2 in some conditions: As mentioned in section 4.1, 2nd harmonic of a GSM signal has a constant amplitude. Suppose before window operation, time-domain GSM samples have unit power level, Figure 5.7 and 5.8 present the GSM power level after testing windowing scheme1 at two extreme frequencies, respectively. (In Figure 5.7 GSM harmonic is located in the middle of subcarrier bins, in Figure 5.8 GSM harmonic is located at subcarrier bin).
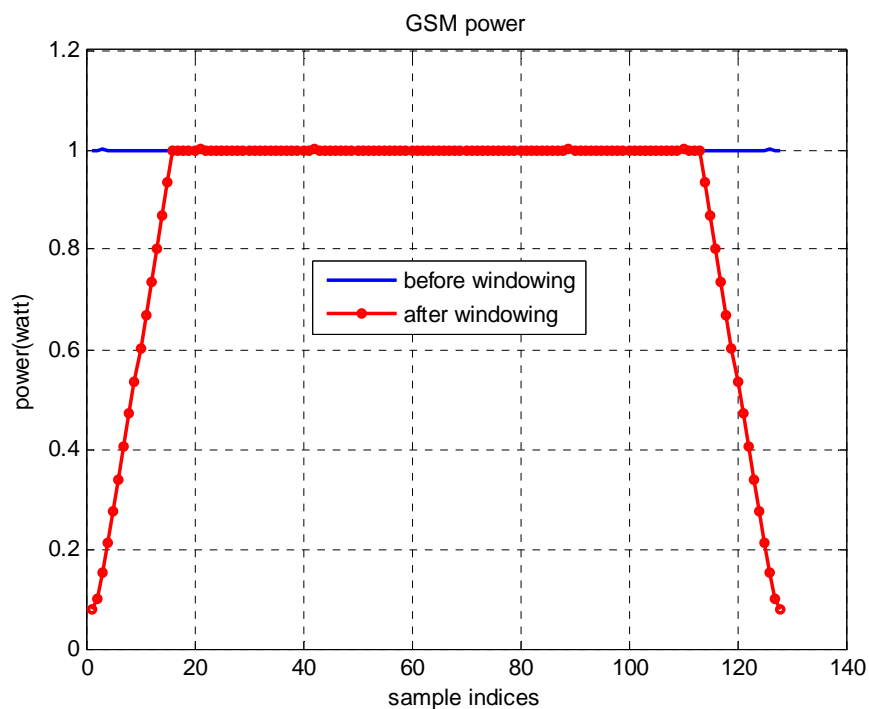
Figure5.7 GSM interference is located in the middle of subcarrier bins

From Figure 5.7 it can be concluded that, when GSM harmonic is located in the middle of subcarrier bins, the windowing operation not only lowers the sidelobes of GSM spectrum, but also decreases the GSM power. However, when GSM harmonic is located at subcarrier bin, the windowing operation increases the GSM power as shown in Figure 5.8, hence degrading the system PER performance. The tendency is also found in the simulation: when GSM frequency is close to the middle of subcarrier bins, windowing operation will decrease GSM power; when GSM frequency is close to subcarrier bins, windowing operation will increase the GSM power. For 3rd WLAN harmonic, in the simulation it is found that, windowing operation will always increase WLAN power at different frequency on the average.
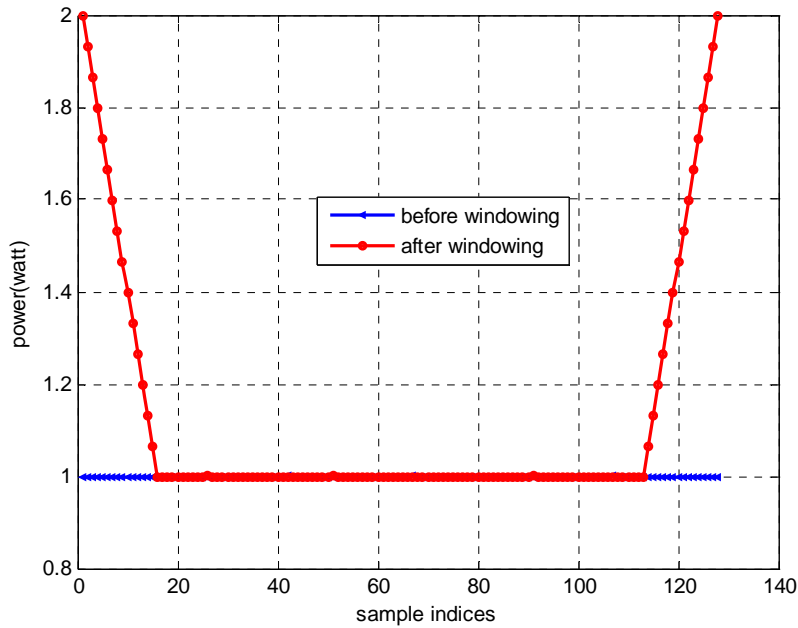
Figure5.8 GSM interference is located at subcarrier bin

To summarize, testing windowing scheme1 can suppress the NBI sidelobes without changing the useful OFDM signal. However the windowing operation will increase the NBI power at certain NBI frequencies, hence will do harm to the system PER performance. The overall effect of windowing scheme1 depends on the comprehensive function of lower sidelobes of NBI spectrum (improving PER performance) and the increased NBI power at certain frequencies (degrading PER performance).

Testing Windowing Scheme2

Testing windowing scheme2 is shown in Figure 5.9, the window is constructed within the OFDM symbol, L is the window width, L can be selected from 0 to 128, and the triangular window shape can be replaced by other standard window shapes, such as constant, and hamming (raised cosine) etc. In this scheme, the window shape has lower sidelobes than rectangular window, and NBI power is lost in part1 and2, however the useful OFDM signal is also corrupted in part1 and2. In the simulation it is found in both weak and strong NBI environment, the windowing scheme always degrades the system performance or brings little benefit. Therefore, we do not analyze this window shape in detail.
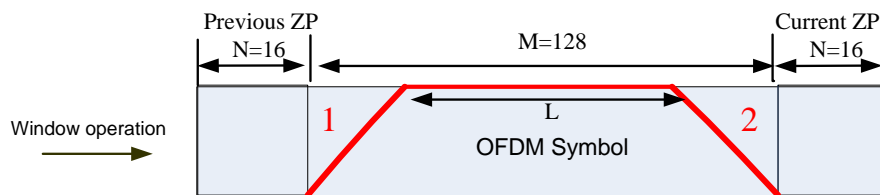
Figure5.9   Testing windowing scheme2

Testing Windowing Scheme3

Test windowing scheme3 is presented in Figure 5.10. The number marked parts: part1, 2, 3, 4 refer to 4 same-shaped triangles respectively. In this example, we use 16 samples from previous ZP and current ZP respectively to extend the traditional rectangular window. The length of OFDM symbol is M . $w(n)$ and $1-w(n)$ are the window coefficients in part1+part4 and part2+part3, respectively. The three step windowing operation are similar as scheme1, the only differences are adding part1 to part2 and adding part3 to part4 before FFT.
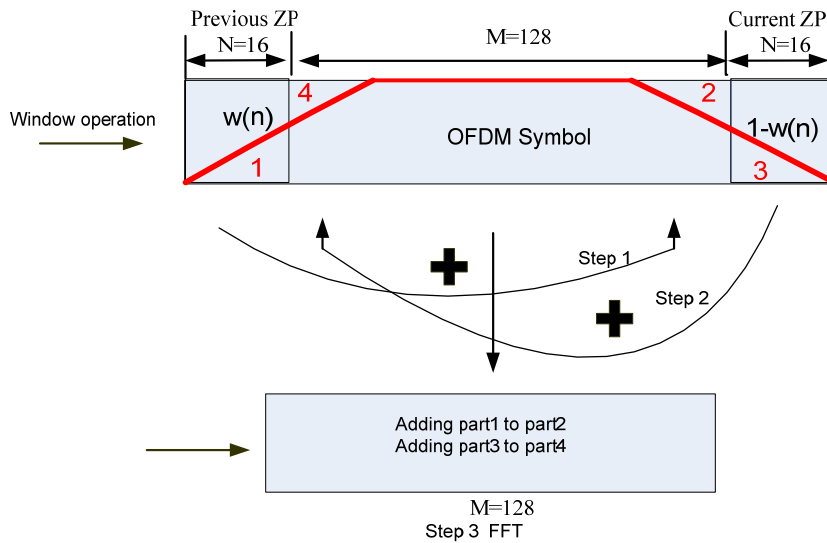
Figure5.10 Testing windowing scheme3

The triangular window shape in Figure 5.10 can be replaced by other standard window shapes, such as constant, and hamming (raised cosine) etc , as shown in Figure 5.11. The corresponding spectrums for different windowing shapes are presented in Figure 5.12, the triangular and hamming windows have lower sidelobes than rectangular window. Compared to scheme1, adding the part1/3 to part2/4 can guarantee the NBI power loss at different NBI frequency (the reason will be explained in section 5.4), the cost paid is the OFDM signal corruption in part2 and part4. In the simulation it is found, in the strong NBI environment (SIR<-10dB), testing windowing scheme3 will improve the PER performance.

To summarize, three testing windowing schemes are introduced in this section. Testing windowing scheme2 is first eliminated, because it degrades the PER performance in both weak and strong NBI environment. Then let us investigate scheme1, it can lower the sidelobes of NBI spectrum, however it increases the GSM interference power (when GSM frequency is close to the subcarrier bins) and WLAN interference power, as a result the overall effect of windowing scheme1 depends on the comprehensive function of lower sidelobes of NBI spectrum (improving PER performance) and the increased NBI power in certain conditions (degrading PER performance). For test windowing scheme3, it can lower the sidelobes of NBI spectrum and reduce the NBI power, the cost paid is the OFDM signal corruption. The testing windowing scheme3 shown in Figure 5.10 is fixed

(suppose the windowing width N does not change), in the simulation we find when adjusting the height of the four same-shaped triangles in Figure 5.10, the modified windowing may have better PER performance under same NBI condition. Hence a new receiver windowing is motivated based on scheme3, the motivation of new windowing is try to find the best trade-off among lower sidelobes, NBI power loss and OFDM signal corruption. In the Chapter6, we will compare the windowing scheme1 and proposed receiver windowing to judge which is better.
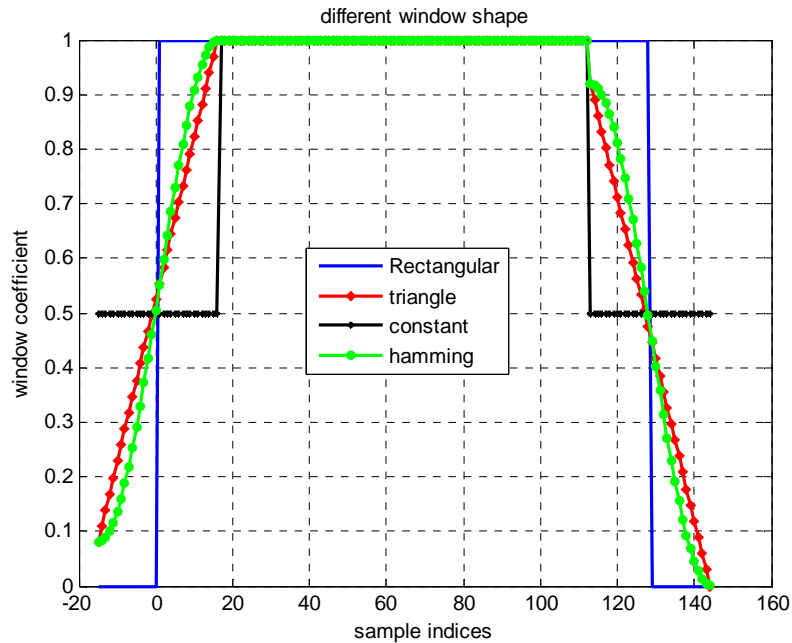
Figure5.11 Different windowing shapes for scheme3
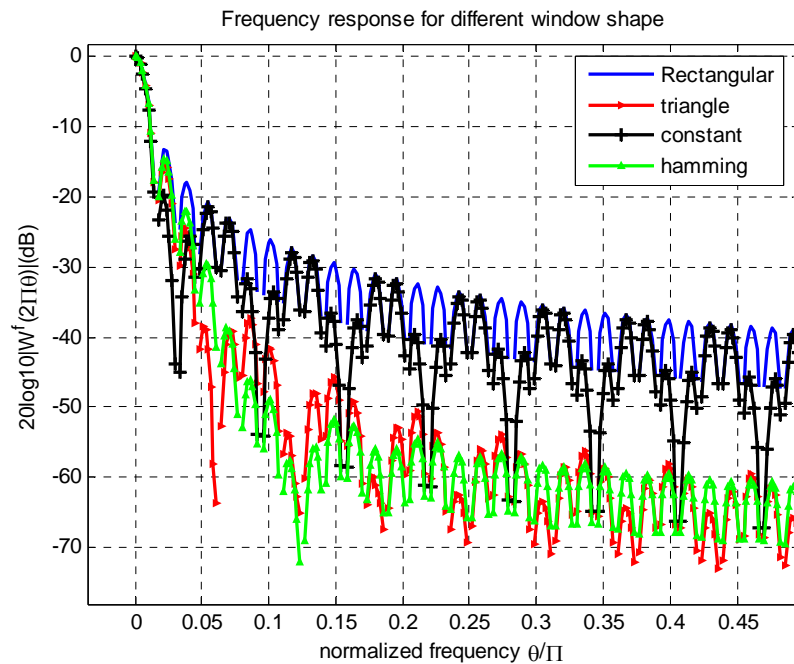
Figure5.12 Different spectrums for scheme3

5.4 Proposed Receiver Windowing

5.4.1 Windowing Shape

The proposed receiver windowing is shown in Figure 5.13. The number marked parts: part1, 2, 3, 4 refer to 4 same-shaped triangles respectively. h is the triangle height, $0 \leq h \leq 1$. N is the triangle width, which is equal to the length of unaffected ZPS. In the AWGN channel, all the ZPS is unaffected, and there is no ISI. The length of OFDM symbol is M. Before windowing operation, cyclical adding is still needed. Then the three steps windowing operations are shown in Figure 5.13:
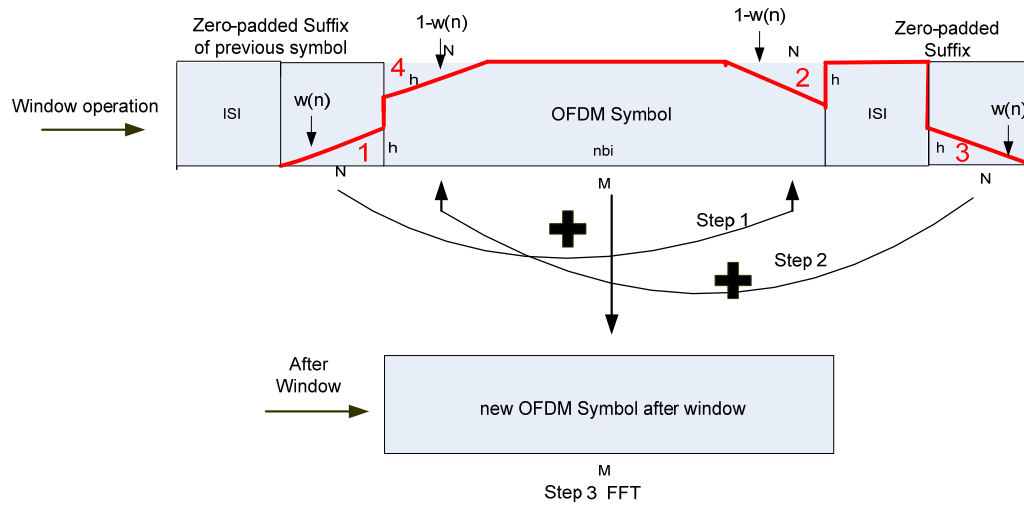
Figure5.13 Proposed Receiver windowing

Step1: Multiplying the N samples of part1 (the unaffected ZPS of previous symbol) by the window coefficients $w(n), n = 1, 2, ...N$, and adding them to the N samples of part2 multiplied by $1 - w(n)$.

Step2: Multiplying the N samples of part3 (the unaffected ZPS of current symbol) by the window coefficients $w(n), n = 1, 2, ...N$, and adding them to the N samples of part4 multiplied by $1 - w(n)$.

Step3: ZPS is removed first, and then the new OFDM symbol is sent to FFT block.

5.4.2 Windowing Design Requirements

In the testing window scheme1, the desired OFDM signal is not corrupted, however scheme1 may result in the increased NBI power at some NBI frequencies. For the new proposed receiver windowing as shown in Figure5.13, the windowing shape can lower the sidelobes of NBI spectrum, also can guarantee the NBI power loss or maintenance

(explained later), but the OFDM signal is corrupted in part2 and part4. The design requirements of the new windowing are try to find the best trade-off among lower sidelobes (windowing benefit), NBI power loss (windowing benefit) and OFDM signal corruption (windowing harm). In the following, these three factors are analyzed, which base on the assumption that the triangle width N is fixed, only the triangle height can be adjusted (Also the triangle can be replaced by other windowing shapes, such as raised-cosine window):

OFDM Signal Corruption
Some useful OFDM signal in part2 and part4 is lost, which is called OFDM signal corruption. Also the subcarriers lose the orthogonality in the frequency domain which results in the inter-carrier interference (ICI) due to the corruption. The corruption makes the error $e(t)$ in equation 5.3 tend to increase, hence degrades the system performance. In order to minimize the OFDM Signal corruption (also suppress ICI), the triangle height h should be close to 0, thus makes the new windowing return to the traditional rectangular window.

Lower Sidelobes
In [1], different windowing shapes are introduced. The smoother time-domain window results in lower sidelobes in its spectrum. As a result, if lower sidelobes are expected to get, the triangle height h should be close to 0.5, making the windowing shape smoother.

NBI Power Loss
Before investigating the NBI power loss, the two NBI sources (2nd harmonic GSM signal and 3rd harmonic of WLAN signal) should be modeled first.

The 2nd harmonic GSM signal has a very small bandwidth (0.54 MHz) compared to subcarrier spacing (4.125 MHz) of MB-OFDM UWB system. Hence the 2nd harmonic GSM signal can be approximately regard as a monochromatic interference in the system, which is a deterministic model as mentioned in section 4.2. In the simulation, different long 2nd harmonic GSM sequences are generated and checked (10^5 samples for each signal sequence with same sampling time). The different sequences have the same periodic and deterministic signal samples. The real and imaginary parts of 2nd harmonic GSM signal are both sinusoid waves.

The 3rd harmonic of WLAN signal can be modeled as a wide-sense stationary (WSS) random process. A WSS process should satisfy two conditions: (1) the mean μ and the variance σ^2 are time-independent; (2) autocorrelation depends only on the time-distance between the pair of values. As mentioned in section 4.2, the 3rd harmonic of a WLAN signal has zero mean and constant variance, so it conforms to the first condition (in the simulation we also verify the mean and variance of different WLAN sequences). Then WLAN autocorrelation function is checked. In the autocorrelation function test, different long 3rd harmonic of WLAN signal (10^5 samples for each signal sequence with same sampling time) are generated. It is found different WLAN sequences have different signal samples, however each sequence has a same autocorrelation function which only depends

on the time-distance between the pair of samples, hence it satisfies the second condition. Figure 5.14 shows the normalized autocorrelation function of 3rd WLAN harmonic, it is close to the autocorrelation function of AWGN due to its relatively large bandwidth (60 MHz). The autocorrelation is 1 at zero point and very small (close to 0) at other time-domain lag indices.
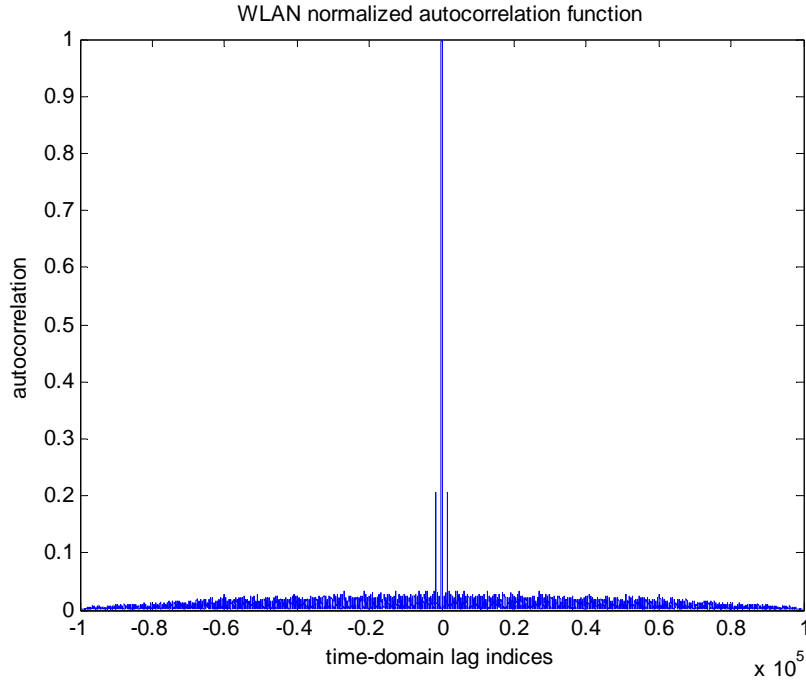
Figure5.14 WLAN normalized autocorrelation function

After introducing the NBI models in the MB-OFDM UWB system, the NBI power loss is analyzed. The NBI power loss caused by step1 and step2 in Figure 5.13 based on the same principle, hence for simplicity, in the following we only explain the working principle of step1, as shown in Figure 5.13. $nbi1(n)$ and $nbi2(n), n = 1, 2, ...N$, refer to the N narrowband interference samples in part 1 and 2, respectively.
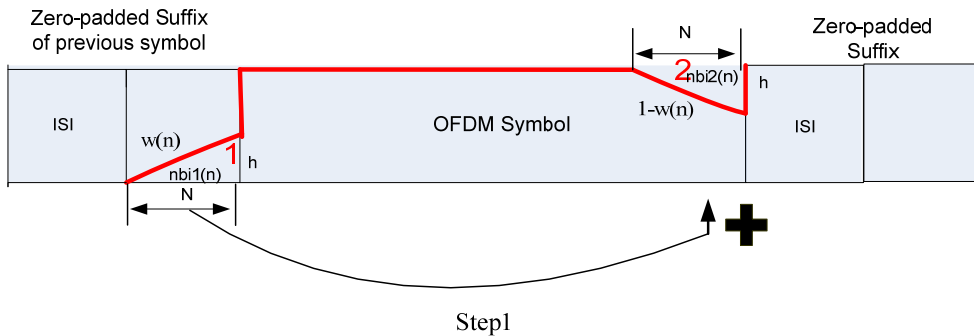
Figure5.15 Step 1 of the Proposed Receiver windowing

For GSM and WLAN interference, they both have zero mean and constant variance σ^2_{nbi}, hence the NBI power is equal to the constant variance:

$$E[|nbi(t)|^2] = D[nbi(t)] = \sigma_{nbi}^2(t) = \sigma_{nbi}^2 \qquad (5.4)$$

where $nbi(t)$ is the complex continuous time domain interference, $E[\cdot]$ denotes expected value, $D[\cdot]$ denotes variance value.

The next step we focus on the power of the nth NBI sample in part 2 shown in Figure 5.15, $n = 1, 2, ...N$. After the windowing operation step1, the power of the nth NBI samples in part 2 $\sigma_w^2(n)$ is:

$$\begin{aligned}
\sigma_w^2(n) &= E\{|(w(n) \cdot nbi1(n) + (1-w(n)) \cdot nbi2(n))|^2\} \\
&= E\{(w(n) \cdot nbi1(n) + (1-w(n)) \cdot nbi2(n)) \cdot \overline{(w(n) \cdot nbi1(n) + (1-w(n)) \cdot nbi2(n))}\} \\
&= E\{w(n)^2 \cdot nbi1(n) \cdot \overline{nbi1(n)} + (1-w(n))^2 \cdot nbi2(n) \cdot \overline{nbi2(n)}) \\
&\quad + w(n) \cdot (1-w(n)) \cdot (nbi1(n) \cdot \overline{nbi2(n)} + \overline{nbi1(n)} \cdot nbi2(n))\} \\
&= w(n)^2 \cdot E[|nbi1(n)|^2] + (1-w(n))^2 \cdot E[|nbi1(n)|^2] \\
&\quad + w(n) \cdot (1-w(n)) \cdot E[nbi1(n) \cdot \overline{nbi2(n)} + \overline{nbi1(n)} \cdot nbi2(n)] \\
&= w(n)^2 \cdot \sigma_{nbi}^2 + (1-w(n))^2 \cdot \sigma_{nbi}^2 + w(n) \cdot (1-w(n)) \cdot E[nbi1(n) \cdot \overline{nbi2(n)} + \overline{nbi1(n)} \cdot nbi2(n)]
\end{aligned}$$

$$(5.5)$$

where $nbi1(n), nbi2(n)$ refers to the nth NBI complex samples in part 1 and 2 respectively, $\overline{nbi(n)}$ represents the complex conjugate, $w(n)$ is the real window coefficient, $\sigma_w^2(n)$ is the power of the nth NBI samples in part 2 after window.

For the deterministic 2nd harmonic GSM signal sequence, in the simulation it can be found, the power of the nth NBI sample after windowing operation are always small or equal to the original power (due to the complementary windowing coefficients $w(n)$ and $1-w(n)$ in part1 and part2, respectively):

$$\sigma_w^2(n) \leq \sigma_{nbi}^2 \qquad (5.6)$$

For the 3rd harmonic WLAN signal sequence, it is a wide-sense stationary process, therefore it can be concluded:

$$\begin{aligned}
E\{nbi(t_1) \cdot \overline{nbi(t_2)}\} &= R_{nbi}(t_1, t_2) = R_{nbi}(t_1 - t_2) \\
&= R_{nbi}(\tau_{12}) = R_{nbi}(-\tau_{12}) \\
&= E\{\overline{nbi(t_1)} \cdot nbi(t_2)\} \\
&\leq R_{nbi}(0) = \sigma_{nbi}^2
\end{aligned}$$

$$(5.7)$$

where R_{nbi} is the autocorrelation function of NBI, $\tau_{12} = t_1 - t_2$.

$$E\{nbi(t_1) \cdot \overline{nbi(t_2)}\} = R_{nbi}(t_1, t_2) = R_{nbi}(t_1 - t_2)$$
$$= R_{nbi}(\tau_{12}) = R_{nbi}(-\tau_{12})$$
$$= E\{\overline{nbi(t_1)} \cdot nbi(t_2)\}$$
$$\leq R_{nbi}(0) = \sigma_{nbi}^2$$

(5.8)

where R_{nbi} is the autocorrelation function of NBI, $\tau_{12} = t_1 - t_2$.

Suppose the interval (discrete samples) between the nth discrete NBI samples in part1 and the nth discrete NBI samples in part2 is K, K is a integer. Hence the time difference τ between the two discrete NBI samples is:

$$\tau = K \cdot T_s \qquad (5.9)$$

where T_s is the sampling time.

Then equation 5.5 can be simplified to:
$$\sigma_w^2(n) = w(n)^2 \cdot \sigma_{nbi}^2 + (1 - w(n))^2 \cdot \sigma_{nbi}^2$$
$$+ w(n) \cdot (1 - w(n)) \cdot E[nbi1(n) \cdot \overline{nbi2(n)} + \overline{nbi1(n)} \cdot nbi2(n)]$$
$$= w(n)^2 \cdot \sigma_{nbi}^2 + (1 - w(n))^2 \cdot \sigma_{nbi}^2 + 2 \cdot w(n) \cdot (1 - w(n)) \cdot R_{nbi}(\tau)$$

(5.10)

The power reduction of the nth discrete NBI samples in part 2 after the windowing operation is:
$$\sigma_{loss}^2(n) = \sigma_{nbi}^2 - \sigma_w^2(n)$$
$$= \sigma_{nbi}^2 - (w(n)^2 \cdot \sigma_{nbi}^2 + (1 - w(n))^2 \cdot \sigma_{nbi}^2 + 2 \cdot w(n) \cdot (1 - w(n)) \cdot R_{nbi}(\tau))$$
$$= 2 \cdot w(n) \cdot (1 - w(n)) \cdot (\sigma_{nbi}^2 - R_{nbi}(\tau)) \geq 0$$

(5.11)

where $\sigma_{loss}^2(n)$ is power loss for the nth NBI samples in part 2, $n = 1, 2, ...N$.

From equation 5.6 and equation 5.11 it can observed, the proposed windowing can guarantee the NBI power loss or maintenance (rarely happen), the value of NBI power loss depends different NBI model. Actually, the AWGN power is also reduced due to the same principle, because the AWGN also can be viewed as a stationary process.

5.4.3 Optimal Windowing Design

In the above section, the effect of three factors is analyzed. When the proposed windowing shape changes, the sidelobes of the NBI spectrum will change accordingly, hence the best trade-off point is not easy to calculate directly. Alternatively we use PER simulation under different SIR to search the optimal triangle height h (the triangle width N is equal to 16 in the simulation), which is shown in Figure 5.16. (In the simulation it was also found that, for the proposed windowing, triangular and raised-cosine window shapes have little difference with the same height and width, that is because some sidelobes of triangle is larger than raised-cosine window, some are smaller, as shown in Figure 5.12).
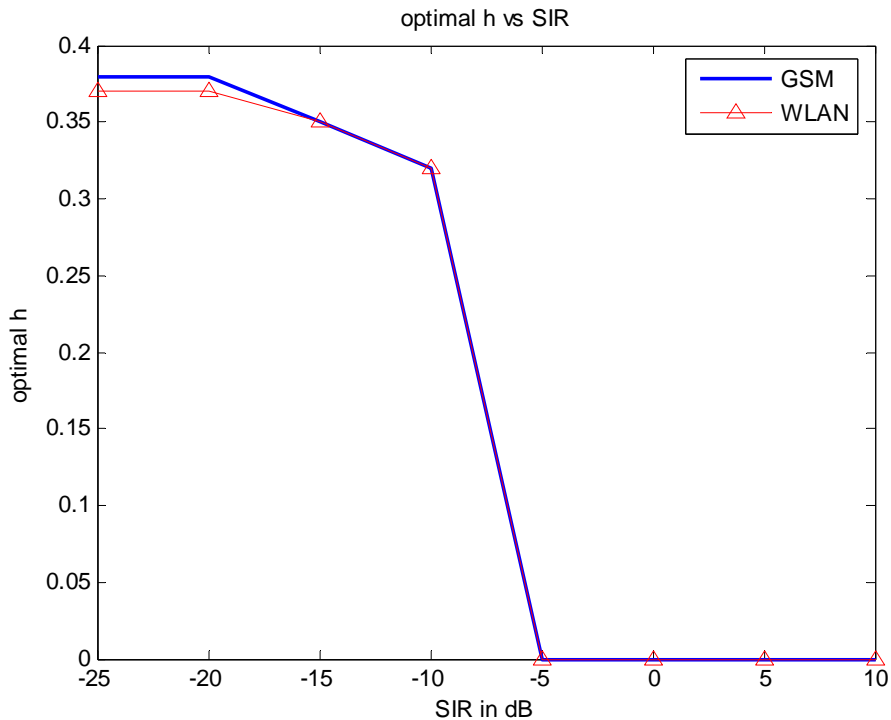
Figure5.16 Optimal h vs. SIR curves

From Figure 5.16 it can be observed that, both for GSM and WLAN interference, the optimal h is close to 0 when SIR is larger than -5dB. It conforms to the windowing design objectives that: In the weak NBI environment, although receiver windowing can lower the sidelobes, the NBI is so weak that can not change the PER performance. In this case, we do not want to lose any useful OFDM signal, the optimal h return to 0. In the strong NBI environment (SIR<-10dB), the optimal h presents the best trade-off among lower sidelobes, NBI power loss and OFDM signal corruption. In the simulation it was also found that, when SIR is between -5dB and -10dB, the optimal windowing at most brings 0.5dB SIR gain. Hence for simplicity, in the real implementation, we can set $h = 0.37$ when SNR<-10dB and h =0 when SNR>-10dB.

5.5   Conclusions

In this chapter, the principle of different windowing design is presented. The windowing technique together with tone nulling can be chosen as the mixed interference to combat strong NBI. In the next chapter, we will compare the PER performance between the proposed windowing and testing windowing scheme1 in the presence of different NBI models, respectively.

References
[1] Digital signal processing (4th edition), Prentice Hall, John G..Proakis, Dimitris G.Manolakis

Chapter 6.   PER performance for the MB-OFDM UWB System

In this chapter, the testing channel models for MB-OFDM UWB system (AWGN channel and IEEE 802.15.3a channel models) are introduced first. Then, the PER requirement and confidence interval for MB-OFDM UWB system are introduced. Finally the proposed windowing and testing windowing scheme1 are applied to test the packet error rate (PER) performance in the presence of different NBI respectively.

6.1   Channel Models

In this section, we introduce the testing channel models for MB-OFDM UWB system.

AWGN Channel

The AWGN channel is the simplest channel model used in most communication systems. The thermal noise in the receivers can be characterized as an additive white Gaussian process. AWGN has a uniform spectral density (making it white), and a Gaussian probability distribution. This model does not account for the phenomena of fading, frequency selectivity, interference, nonlinearity or dispersion.

IEEE 802.15.3a channel models

In order to evaluate different Physical (PHY) layer proposals, IEEE 802.15.3a channel modeling sub-committee proposed four channel models (CM1, CM2, CM3, and CM4) for realistic UWB environments [1]. These models are derived from the well-known Saleh-Valenzuela (SV) model [2] with slight modifications. Each channel model has an exponential decay profile, also the overall power of each channel exponentially decays with time. As given in [1], four different sets of parameters are chosen to represent different channel conditions in typical usage scenarios where IEEE 802.15.3a devices are expected to operate (office and residential as well as LOS and NLOS as a function of distance). The sampling time of our UWB system is 1/(0.528) nsec. The average power decay profiles for each channel model based on this sampling time are shown in Figure 6.1.

6.2   SIR vs. SNR curve

As introduced in Chapter 3, the MB-OFDM UWB system is required to operate under PER=8% with a PSDU of size 1024 octets. In the simulation we provide a single curve of SIR vs. SNR that represents PER=8%, as shown in Figure 6.2. The area above this curve indicates the system can work under PER<8%.
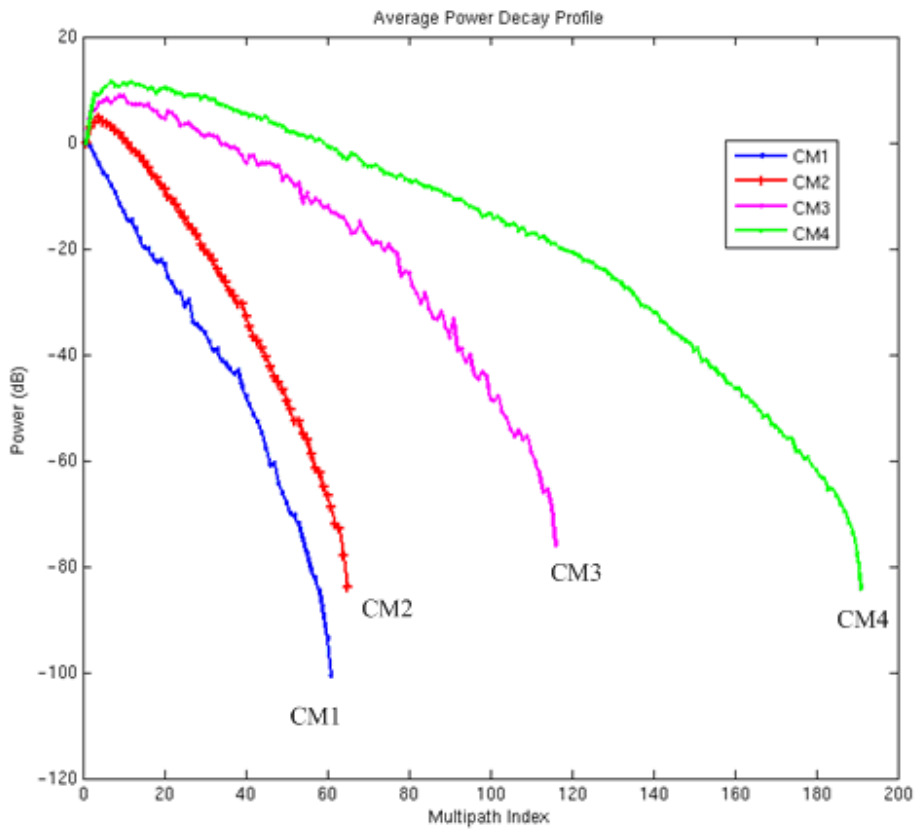
Figure6.1 CM1-CM4 average power decay profile
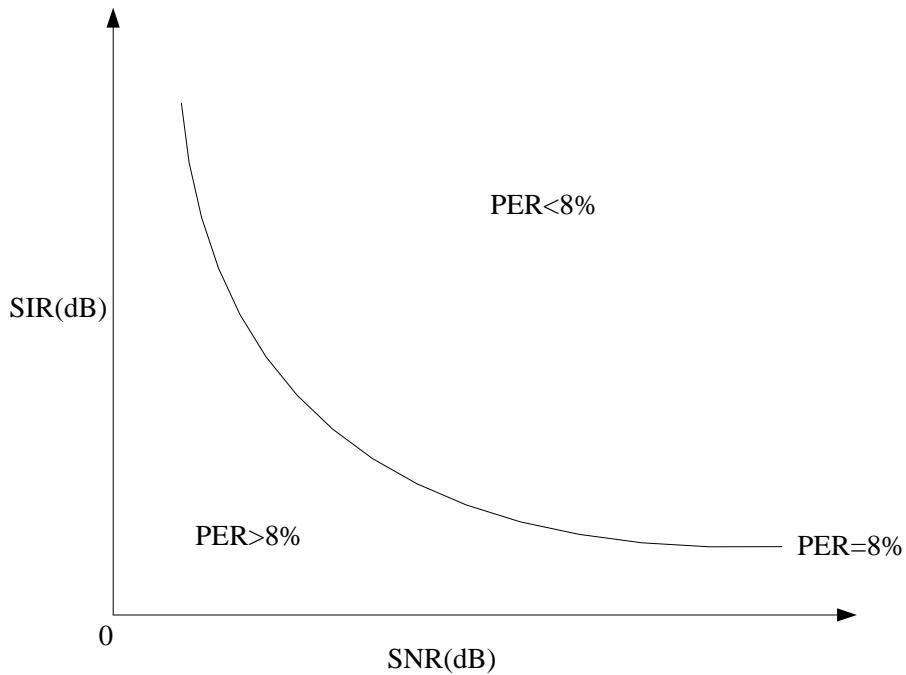
Figure6.2 SIR vs. SNR curve when PER=8%

6.3 Confidence Interval

As mentioned in section 3.8, the MB-OFDM UWB system is required to operate under PER=8% with a PSDU of size 1024 octets. In this section, the concept of confidence interval is presented, which is used to indicate the reliability of PER estimation.

After the receiver side of system, the unscrambled PSDU sequence is received. If the PSDU is successfully received, 0 is used to represent the correctness with possibility p ; On the contrary, if the PSDU is failed (as long as one bit is not the same as the transmitted PSDU), 1 is used to represent the error with possibility $1-p$ .So the expected error rate for a PSDU transmission is equal to:

$$E(\mathrm{X}) = \sum_i x_i p_i = 0 \cdot p + 1 \cdot (1-p) = 1-p \tag{6.1}$$

where $E[\cdot]$ denotes expected value, X is the random variable PSDU, x_i denotes the PSDU is successfully received or failed, p_i is the probability for successfully received or failed, correspondingly.

The variance of error rate for a PSDU transmission is:

$$Var(X) = E\left((X - E(\mathrm{X}))^2\right) = E[\mathrm{X}^2] - [E(\mathrm{X})]^2$$
$$= \sum_i (x_i)^2 p_i - (\sum_i x_i p_i)^2 = 0^2 \cdot p + 1^2 \cdot (1-p) - (1-p)^2 \tag{6.2}$$
$$= (1-p) - (1-p)^2 = p - p^2 = p(1-p)$$

As we know if a is a constant,

$$E(aX) = aE(X) \tag{6.3}$$
$$Var(aX) = a^2 Var(X) \tag{6.4}$$

If X_n are independent PSDU variables, the variance of the sum of uncorrelated PSDU is the sum of their variances:

$$Var(\sum_n X_n) = \sum_n Var(X_n) \tag{6.5}$$

So the mean and variance of the PSDU transmission error rate are:

$$E(\overline{X}) = E(\frac{1}{N} \sum_{n=1}^{N} X_n) = \frac{1}{N} \cdot \sum_{n=1}^{N} E(X_n)$$
$$= \frac{1}{N} \cdot N \cdot (1-p) = 1-p \tag{6.6}$$

$$Var(\overline{X}) = Var(\frac{1}{N} \sum_{n=1}^{N} X_n) = \frac{1}{N^2} \cdot \sum_{n=1}^{N} Var(X_n)$$
$$= \frac{1}{N^2} \cdot N \cdot p(1-p) = \frac{p(1-p)}{N} \tag{6.7}$$

Applying the central limit theorem, while assuming that N is sufficiently large, the X_n is a normal distribution:

$$X_n \sim N(\mu, \sigma^2) = N(1-p, \frac{p(1-p)}{N})$$ (6.8)

where μ is mean and σ^2 is standard deviation squared.

$$\sigma^2 = Var(\overline{X}) = \frac{p(1-p)}{N} \Rightarrow \sigma = \sqrt{\frac{p(1-p)}{N}}$$ (6.9)

In statistics, the 68-95-99.7 rule states that for a normal distribution, almost all values lie within 3 standard deviations of the mean. About 95.4% of the values lie within 2 standard deviations of the mean (or between the mean minus 2 times the standard deviation, and the mean plus 2 times the standard deviation). The statistical notation for this is: $\mu \pm 2\sigma$ [3].

$$\mu \pm 2\sigma = [(1-p) - 2\sqrt{\frac{p(1-p)}{N}}, (1-p) + 2\sqrt{\frac{p(1-p)}{N}}]$$ (6.10)

Suppose $\mu + 2\sigma = (1-p) + 2\sqrt{\frac{p(1-p)}{N}} < 8\%$, this means there is 1-2.3%=97.7 % sure that $(1-p) < 8\%$, as shown in Figure 6.3. In the packet error rate simulation, we use this confidence interval to make sure that, there is 97.7 % guarantee that system can work under PER<8%. In the simulation, at least 100 PSDU should be transmitted to estimate the PER of system.
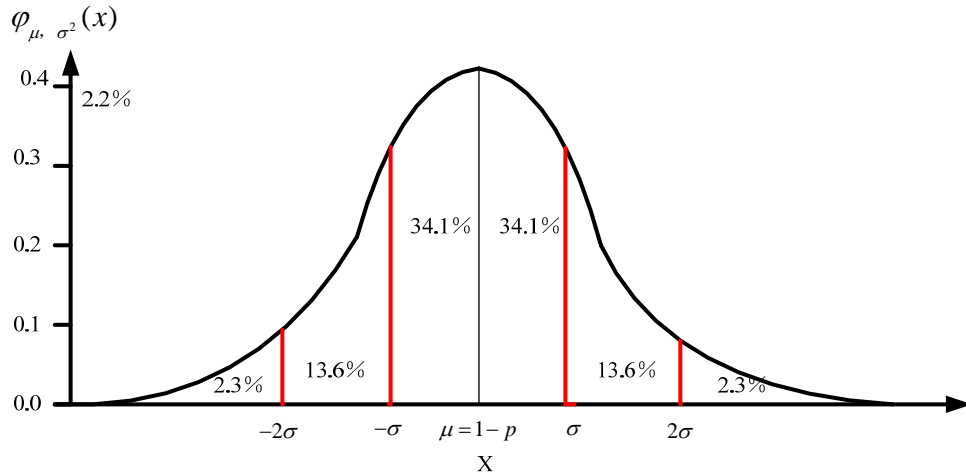
Figure6.3 Standard deviation and confidence intervals

6.4   Simulation Result

To evaluate the mixed NBI cancellation scheme on MB-OFDM UWB system, we run simulations with the configuration parameters in Table 6.1.

Constellation	QPSK
Channel model	AWGN
Data rate	53.3 Mbps
Payload length	1024 bytes
Channel coding	Convolutional codes($K = 7$, rate 1/3)
Info Bits/6 OFDM Symbols	$N_{IBP6S} = 100$
TDS factor	$N_{TDS} = 2$
Coded Bits/OFDM Symbol	$N_{CBPS} = 100$
Cyclic Interleaver	$N_{cyc} = 33$
NBI model	2nd harmonic of GSM signal with 0.54MHz bandwidth 3rd harmonic of WLAN signal with 60MHz bandwidth
Synchronization	Perfect
LLR Calculation	Euclidean distance
AGC	Optimally scaled
ADC	6-bit ADC
Viterbi decoding	Soft decision
Window width	16
Window height	SNR<-10dB , h =0.37; SNR>-10dB , h =0

Table 6.1 Simulation Configuration of MB-OFDM System

6.4.1 PER under GSM Interference

As discussed in section 4.3, GSM interference frequency largely influences the spectrum leakage degree. In the simulation, we test the windowing effect (proposed windowing and test windowing scheme1) on two extreme frequecies: (A) GSM interference is located at subcarrier bin frequency (B) GSM interference is located in the middle of two adjacent subcarriers. The PER performance is simulated in the weak and strong GSM interference environments, respectively.

Weak GSM locates at bin frequency

When only using windowing to combat GSM interference (GSM locates at bin frequency), the system can tolerate relatively weak NBI (SIR>8.5dB) under PER<8% constrain. The windowing design objectives have been discussed in section 5.1, actually in the weak NBI environment, there is no need to implement the receiver windowing, because NBI energy on the sidelobes is so weak that can not affect the OFDM signal. Figure 6.4 verifies the objectives, the two windowing approaches can not bring any benefit or even do harm to the system. For the new proposed windowing, when SIR>-10dB the optimal h is 0, hence there is no difference compared to the traditional rectangular windowing. For test windowing scheme1, when GSM locates at bin frequency, the windowing operation increases the interference power (the increased power overweighs the lower sidelobe), hence decreasing the PER performance.
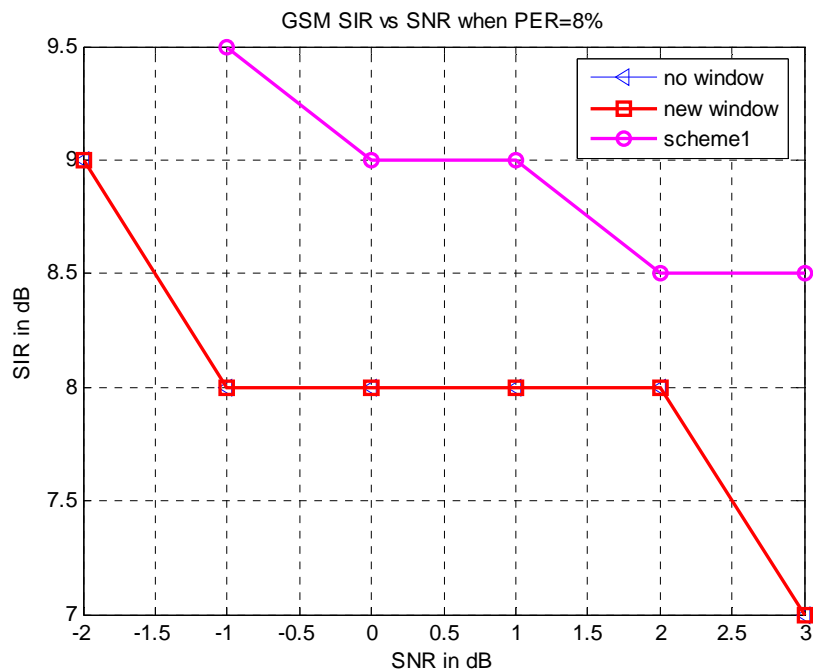
Figure6.4 weak GSM locates at the 31st subcarrier

Strong GSM locates at bin frequency

When using the mixed NBI cancellation scheme to combat strong GSM interference (tone nulling is applied to cancel the main lobe energy and windowing is used to lower the NBI sidelobes), the benefit of windowing becomes obvious. As explained in section 4.3, when GSM interference is located at subcarrier bin frequency, the main NBI energy concentrates on its central subcarrier, in this case, only one subcarrier is used for tone nulling. Figure 6.5 shows the windowing effect under strong GSM interference. The new windowing brings the benefit but not large (from 0dB to 1dB), it is because when GSM interference is located at subcarrier bin frequency, little GSM energy is leaked to other neighboring subcarriers. The test windowing scheme1 seriously degrades the PER performance (from 13dB to 14dB according to different SNR) due to the increased GSM interference power.

Weak GSM locates in the middle of bin frequencies

Figure 6.6 shows the windowing effect under weak GSM environment when the interference locates in the middle of bin frequencies. The test windowing scheme1 improves the PER performance. However, the benefit is so small that can be neglected in the weak GSM environment.
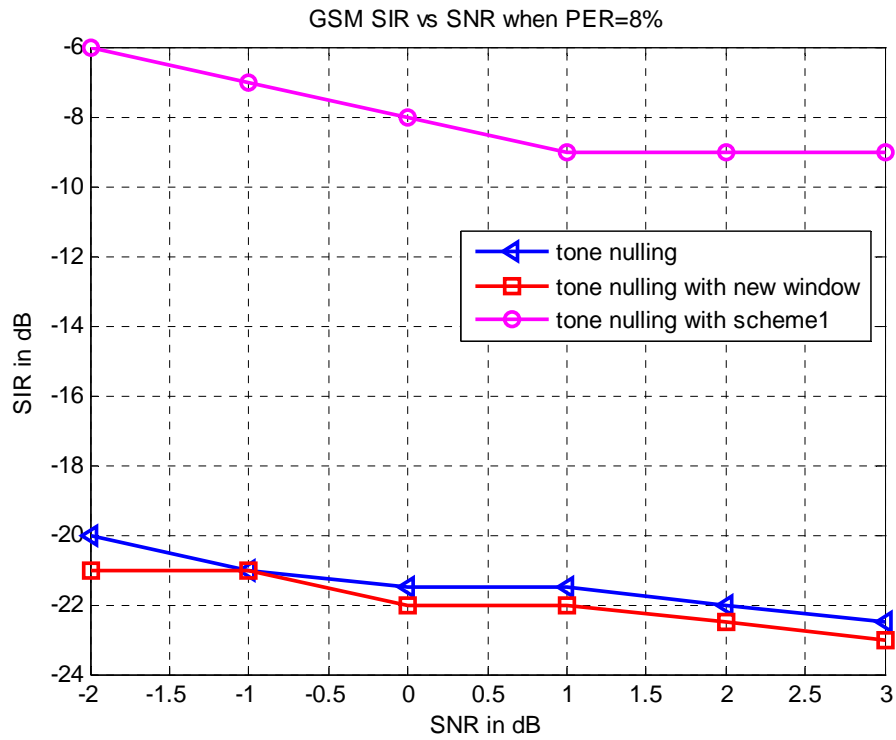
Figure6.5 strong GSM locates at the 31st subcarrier
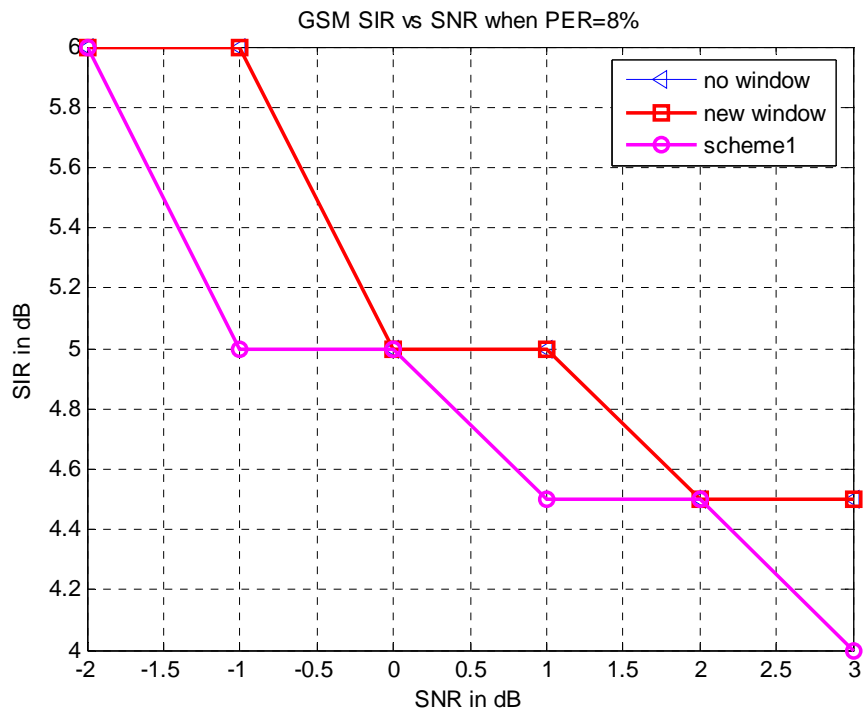
Figure6.6 weak GSM locates at the midpoint between subcarrier 31 and 32

Strong GSM locates in the middle of bin frequencies

When using mixed NBI cancellation scheme, the windowing benefit is obvious under strong GSM environment. When GSM interference is located in the middle of subcarrier bins, spectrum leakage phenomenon are most serious, in this case 30 subcarriers are used for tone nulling. The simulations results are shown in Figure 6.7. For the new windowing, it can improve the PER performance from 8dB to 9.5dB according to different SNR. For test windowing scheme1, the SIR gain is larger, 10dB to 13dB. It is because when GSM interference is located in the middle of subcarrier bins, scheme1 can lower the GSM sidelobes and decrease the GSM power without corrupting the OFDM signal. The tendency can be concluded from the simulation result: when SNR is improving, meaning that the system can tolerate more NBI under PER<8% constrain, the SIR gain increases after windowing. We can expect that when we properly increase the tone nulling number or using two stage NBI cancelation scheme (notch filter together with tone nulling) to tolerate stronger NBI , the SIR gain brought after windowing will further increases.
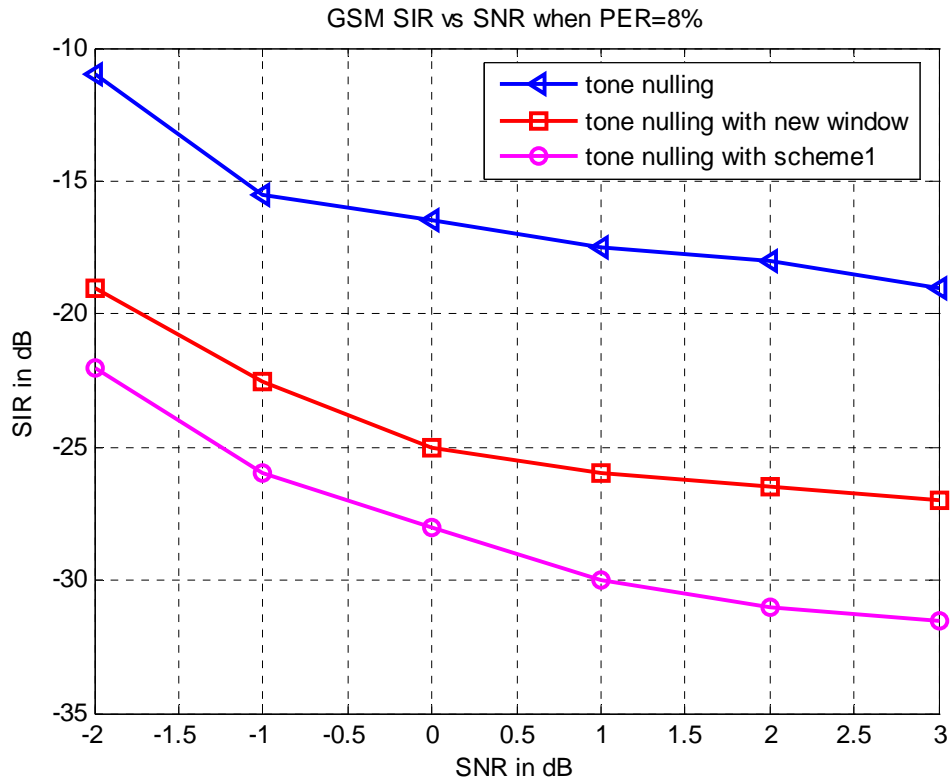
Figure6.7 strong GSM locates at the midpoint between subcarrier 31 and 32

6.4.2 PER under WLAN Interference

After testing the windowing effect on GSM interference, we will test another extreme NBI model with the largest bandwidth: 3rd harmonic of WLAN interference. As explained in the section 4.3, the PSD shapes of WLAN interference are almost the same

at different frequencies, therefore the PER under WLAN interference can be tested at a random location. Figure 6.8 and 6.9 show the SIR vs. SNR curve under weak and strong WLAN environments, respectively.

Weak WLAN environment

Figure 6.8 shows the effect of new proposed window and test windowing scheme1 under weak WLAN environment. In this case, the optimal h for the new proposed windowing is 0, hence the windowing performance is the same as traditional rectangular window. For scheme1, the increased WLAN power degrades the PER performance, but the deterioration is not much (0dB to 0.5dB).
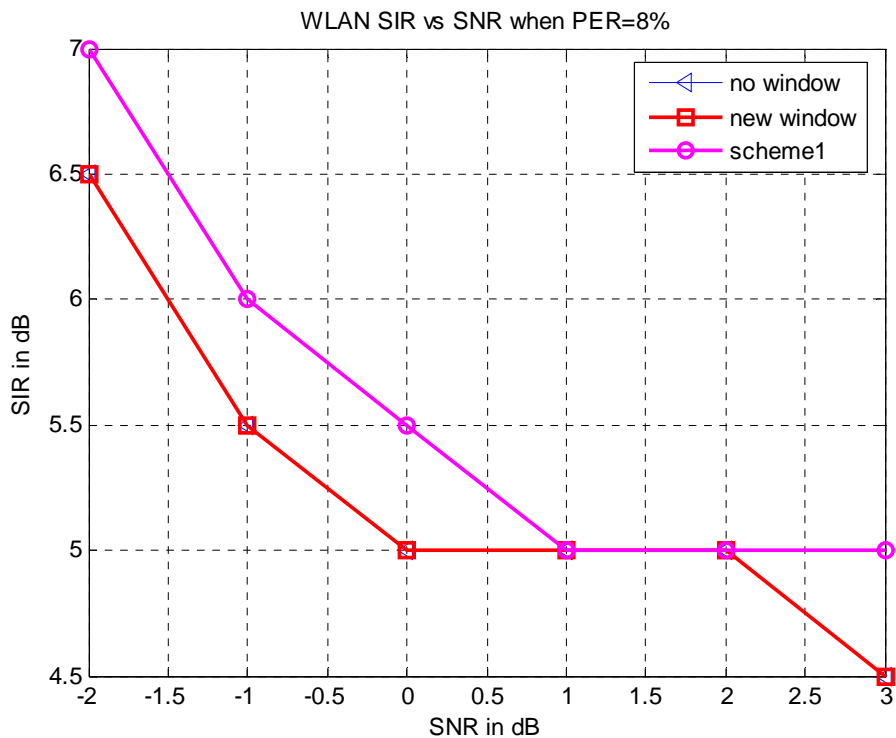
Figure6.8 Weak WLAN environment

Strong WLAN environment

Figure 6.9 presents the windowing effect when using the mixed NBI cancellation scheme to combat strong WLAN interference. The new proposed window and test windowing scheme1 both improve the PER performance. For new proposed window, lower spectrum sidelobes and WLAN power loss overweigh the impact of corrupted OFDM signal. For test windowing scheme1, the lower spectrum sidelobes overweighs the increased WLAN power. From the simulation results it can be observed that, new windowing has larger SIR gain compared to test windowing scheme1.
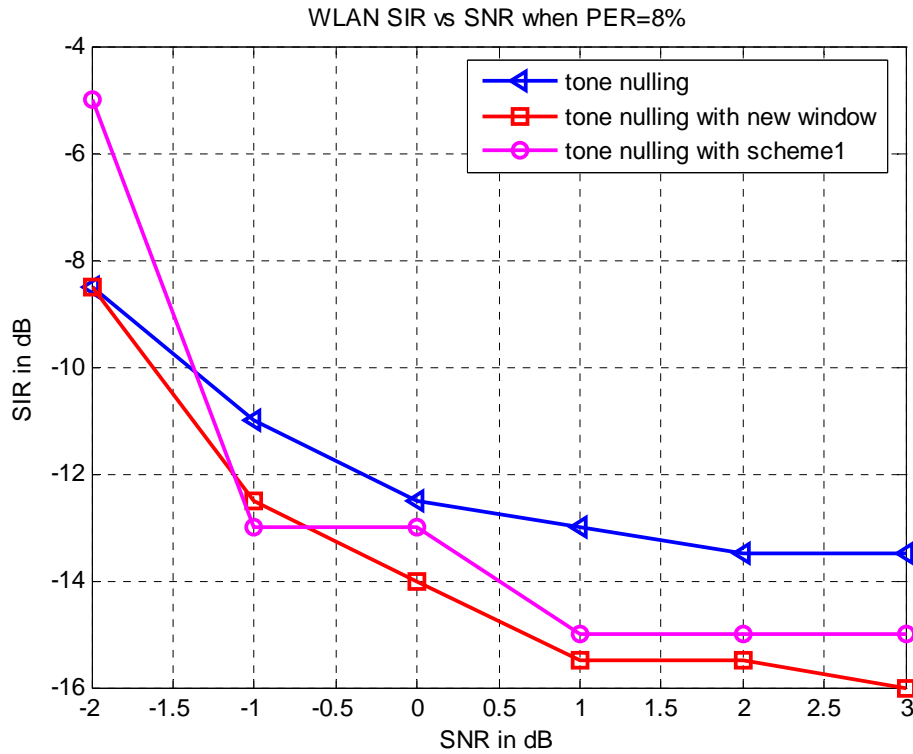
Figure6.9 Strong WLAN environment

6.4.3 PER under Fading Channel

In the simulation it is found that, when only using tone nulling to combat NBI under fading channel, the maximum allowable SIR is larger than 15dB under PER<8% constrain, in this case there is need to implement the receiver windowing. However, we can expect the new proposed windowing may bring some benefit when UWB system using two or more stages NBI cancelation scheme (notch filter together with tone nulling) to combat strong NBI. Because in Figure 6.1, it can be observed that for CM1 and CM2, the main energy concentrate on the first 20 multipath components (the first 20 multipath components in CM1 occupy 99.72% energy and in CM2 occupy 98.06% energy), hence the ISI influence from the 21st multipath component can be can neglected, and there still 16 unaffected ZPS samples can be used for the receiver windowing construction.

6.5 Conclusions

In this chapter, we compared the PER performance between the proposed new window and testing windowing scheme1 under 6 cases (two NBI models with different frequencies, two NBI environments). It is observed that only in one case (strong GSM interference locates in the middle of subcarrier bins), testing windowing scheme1 has obvious advantage than proposed new window.

References

[1] "Channel Modeling Sub-committee report final," J. Foerster, Ed, IEEE P802.15-02/490r1-SG3a, February 2003.

[2] "A Statistical Model for Indoor Multipath Propagation," A. Saleh and R. Valenzuela, IEEE JSAC,Vol. SAC-5, pp. 128-137, Feb. 1987.

[3] http://en.wikipedia.org/wiki/68-95-99.7_rule

Chapter 7. Conclusions and Future work

7.1 Conclusions

In this thesis, the narrowband interference in the MB-OFDM UWB system has been discussed. Basic concepts of OFDM systems and ECMA-368 MB-OFDM UWB system are introduced in the first part of this thesis. Then NBI models, spectrum leakage and NBI impact in the MB-OFDM UWB system are presented. In the analysis, we limit ourselves to the 2nd harmonic of GSM interference and 3rd harmonic of WLAN interference, which have the minimum and maximal bandwidth respectively. Later, the existing NBI cancellation/mitigation approaches have also been investigated. After a comprehensive comparison among them, a mixed NBI cancellation scheme is proposed, which combines tone nulling and receiver windowing techniques to combat strong NBI in the system. Finally a new receiver windowing for the mixed NBI cancellation scheme has been presented. The performance of receiver windowing is shown by SIR vs. SNR curve simulations.

The main contribution of this thesis is to propose a new receiver windowing for NBI mitigation in the ZP-OFDM systems, because the current receiver windowing techniques are only suitable for CP-OFDM scheme. Compared to other NBI cancelation approaches in chapter 4, receiver windowing technique has its unique advantages: low design complexity; no need for NBI detection (particularly important under multi-interferers situations); no need to be redesigned. These merits make windowing technique a promising NBI mitigation approach. Also the new windowing technique has its limitations: windowing only takes obvious effect in the strong NBI environments; windowing construction depends on the multipath condition.

7.2 Recommendations for Future Work

We recommend the following future work for the development of an algorithm in the direction of a usable implementation:

• The windowing effects on two extreme NBI cases are tested in the thesis. What are the benefits if the windowing is applied to other NBI models within these two extreme cases?

• Windowing technique can work under multi-interferers situations without the NBI detection. What are the benefits if windowing is implemented under multi-interferers?